

Fluorescent Gold Nanoclusters as a Powerful Tool for Sensing Applications in Cancer Management

Shiji R, Manu M. Joseph, Unnikrishnan BS, Preethi GU and Sreelekha TT

Abstract Fluorescent gold nanoclusters (AuNCs) comprising of several to tens of atoms with a dimension comparable to the Fermi wavelength of electrons have attracted greater attention in chemistry and medicine for the past decade due to their high fluorescence, good photostability, non-toxicity, excellent biocompatibility and water solubility. Green synthesis of AuNCs provides excellent possibilities to use them as biocompatible tools for fluorescent imaging, targeted therapy and have been extensively used in many fields of oncology. Biomolecules or functional molecules capped AuNCs could be further modified by conjugating targeting moieties and therapeutic molecules which allow active targeting, imaging and drug delivery at the tumor site. The current book chapter mainly focuses on the recent reports including mechanism of fluorescence, various synthesis strategies, bioconjugation and application of AuNCs for precise diagnosis and treatment of cancer.

Keywords Cancer · Nanoclusters · Bioconjugation · Imaging · Targeted therapy

Abbreviations

μg	Microgram
μM	Micromolar
A	Adenine
AgNCs	Silver nanoclusters
AML	Acute myeloid leukemia
Au DSNPs	Dendrimer stabilized AuNPs
AuNC@DHLA	Dihydrolipoic acid stabilized AuNCs
AuNCs	Gold nanoclusters
AuNCs@Tyr	L-Tyrosine capped AuNCs
AuNPs	Gold nanoparticles
AuNRs	Gold nanorodes

Shiji R · Manu M. Joseph · Unnikrishnan BS · Preethi GU · Sreelekha TT (✉)
Laboratory of Biopharmaceuticals and Nanomedicine, Division of Cancer Research,
Regional Cancer Centre, Trivandrum 695011, Kerala, India
e-mail: ttsreelekha@gmail.com; ttsreelekha@rcc.gov.in

BGLA	(2-(4-(bis(4-(diethylamino)phenyl)(hydroxy)methyl)phenoxy)ethyl 5-(1,2-dithio-lan-3-yl)pentanoate)
BSA	Bovine serum albumin
C	Cytosine
CD	Cyclodextrin
CSC	Cancer stem cells
CT	Computed tomography
DFT	Density functional theory
DMF	Dimethylformamide
DNA	Deoxy ribonucleic acid
DOX	Doxorubicin
DPA	D-penicillamine
EDC	1-[(3-dimethylamino)-propyl]-3-ethylcarbodiimide hydrochloride
EDTA	Diamine tetra acetate
EGFR	Epithelial growth factor receptor
EPC	Endothelial progenitor cells
EPR	Enhanced permeation and retention
FA	Folic acid
FR	FA receptor
G	Guanine
G ₄ NH ₂	Dendrimers with terminal amine group
G ₄ OH	Dendrimers with terminal hydroxyl group
HAEC	Human aortic endothelial cells
HDAC 1	Histone deacetylase 1
Her	Herceptin
HP-DNAs	Hairpin DNAs
HRP	Horseradish peroxidase
HRP-AuNCs	HRP functionalized AuNCs
ICG	Indocyanine green
Lf	Lactoferrin
LsGFC	Lysozyme-stabilized gold fluorescent clusters
MALDI-TOF MS	Matrix-assisted laser desorption ionization-time-of-flight mass spectrometry
MDR	Multidrug resistance
mg	Miliigram
ml	Milliliter
MPA	Mercaptopropionic acid
MPCs	Monolayer protected AuNCs
MRI	Magnetic resonance imaging
MTX	Methodretaxate
NCA	NP-based contrast agents
NIR	Near-infrared
nm	Nanometer

NPs	Nanoparticles
OCT	Optical coherence tomography
PA	Photoacoustic tomography
PDGF AA	Platelet-derived growth factor AA
PEG	Poly ethylene glycol
PEI	Polyethylenimine
PET	Positron emission tomography
pH	Potential of hydrogen
PKA	Protein kinase A
PTM	Post translational modification
QDs	Quantum dots
QY	Quantum yield
R	Rifampin
RNA	Ribonucleic acid
SERS	Surface-enhanced Raman scattering
SPR	Surface plasmon resonance
ss-DNAs	Single stranded DNAs
sulfo-NHS	Sulfo-N-hydroxysuccinimide
T	Thymine
TAT	Trans-activating transcriptional activator
TB	Tuberculosis
THPC	Tetrakis(hydroxymethyl)phosphonium chloride
TNF	Tumor necrosis factor
TPL	Two-photon luminescence
UV	Ultra violet

1 Introduction

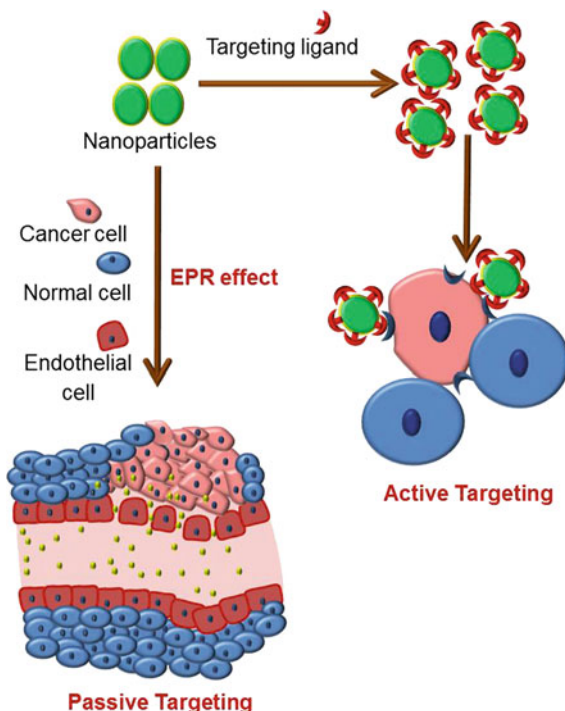
Nanotechnology is a broad term which covers copious regions of science, technology and innovation. It works at atomic, sub-atomic and macromolecular scales wherein, quantum effects dominates and matter behaves differently. The rapid growth of biotechnology in sync with nanotechnology, commonly referred to as nanobiotechnology, is a rapidly flourishing arena that investigates biological systems for the fabrication of new biomaterials using nanoscale principles and techniques (Roco 2003), which could be useful tools for biosensing, cell labeling, molecular imaging, targeted therapy (Qu et al. 2015) and many more. This hybrid science has attained much higher imagination of fiction writers, engineers, scientists and every common individual interested in science. Today, it is estimated that there are more than 1,600 nanotechnology-based products and devices, with new ones entering the business sector at a quick pace. Nanoscale refers to size dimensions typically between approximately 1–100 nm. Even though particles above 100 nm

are also considered as nanoparticles, nanofabrication techniques are increasingly adapted to maintain the size below 100 nm, owing to the unique physicochemical parameters adapted under this range. Any type of a material that has one or more measurements in the nanoscale is considered to be as a nanomaterial (Sekhon 2014).

Cancer, a heterogeneous pathological condition is one among the most feared maladies in cutting edge social orders even though much progress was made in prevention, diagnosis and treatment. Cancer mortality could be abridged by implementing evidence-based strategies and assessment of the progress and suitability of therapies by rapid and non-invasive methods (Gao et al. 2014). Even though early detection had a large scope of cure, too many patients are diagnosed in late or too advanced stage where treatment response is inadequate (Weissleder 2002). Conventional therapies are the foundation of care in any disease conditions and also in cancer. Most people with cancer receive surgery, chemotherapy, radiation therapy, or immunotherapy therapies eventually amid treatment, and numerous will have a mix of these medications. Conventional therapies are constantly evolving and improving, with progresses in science and technology, to advance efficacy while fading destructive side effects. The field of nanotechnology has led to the development of many innovative strategies for effective detection and treatment of cancer by overcoming limitations associated with conventional cancer diagnosis and therapy (Srinivasan et al. 2015). Conventional chemotherapeutic compounds are non-targeting and act as cytotoxic agents which kills actively dividing cancer cells along with other healthy dividing normal cells, which creates significant side-effects on patient longevity and quality of life. Nanoparticles (NPs) have an excellent surface area/volume ratio which will enable them to adhere to tumor niche, moreover they could be surface decorated with cancer-specific molecules (drugs or ligands) which enable them to specifically bind to their targets on the cancer cell. Targeted delivery enables the distribution of drugs specific to the cancer cells, thereby decreasing the systemic toxicity in an accordable manner (Yu et al. 2012; Srinivasan et al. 2015). The difficulties in improving fabrication of nanoparticles custom-made to tumor specific signs still remain; however it can be assumed that nanoscale devices convey critical guarantee towards better approaches in every fields of oncology (Zamboni et al. 2012).

Precise and real time imaging of tumors using NP-based fluorescent probes (Wang et al. 2013) with long circulation times, excellent specificity and non-toxicity will be a boon in oncology. The clinical applications of contrast agents are severely limited due to their short half-lives, their ability to elicit an immune response and the difficulty that they experience with crossing biological membrane (Sivasubramanian et al. 2014). Carefully designed NP-based contrast agents (NCAs) could overcome biological barriers to reach tumors site either through active or passive targeting mechanisms (Ferrari 2005; Couvreur and Vauthier 2006; Peer et al. 2007) and simultaneously deliver both imaging agents and therapeutics. In passive targeting, the leaky vasculature of tumor enables NCA to accumulate via the enhanced permeation and retention (EPR) effect which allows for the extravasation of NPs from the circulation through abnormal fenestrations in tumor

Fig. 1 Mechanism of passive and active targeting. In passive targeting, the leaky vasculature of tumor enables NCA to accumulate via the enhanced permeation and retention (EPR) effect. In active targeting involves the conjugation of targeting ligands or receptors to the surface of the NCA, enabling them to penetrate the cancer cells via receptor-mediated endocytosis

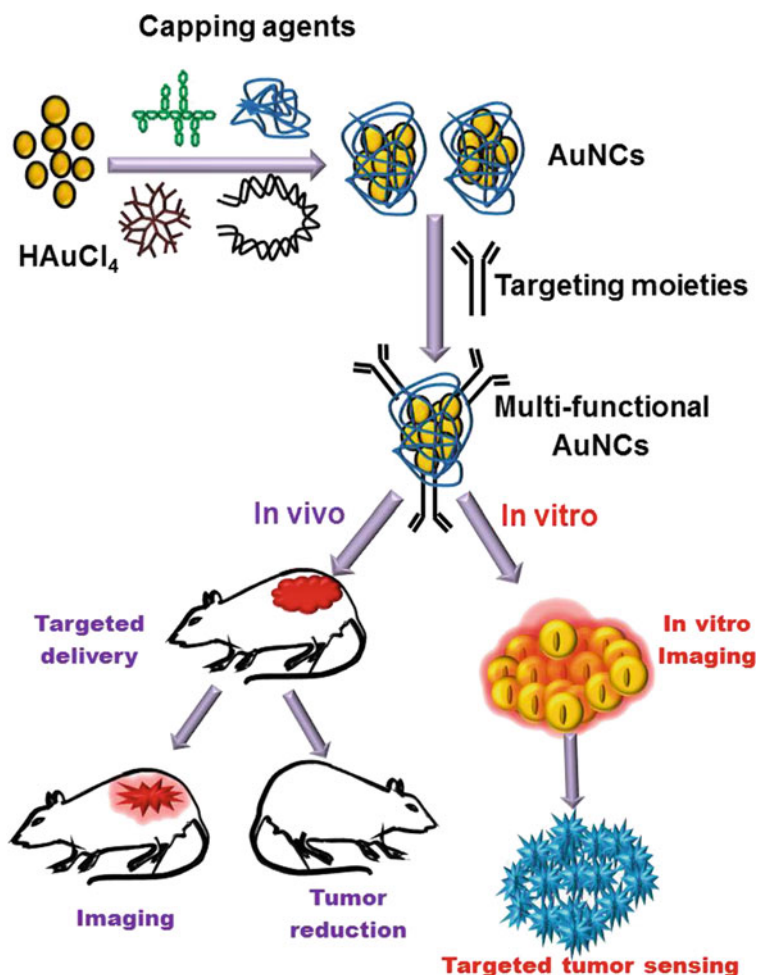


vasculature. Active targeting involves the conjugation of targeting ligands or receptors to the surface of the NCA, enabling them to penetrate the cancer cells via receptor-mediated endocytosis (Saravanakumar et al. 2009; Choi et al. 2010; McCarthy et al. 2010; Sivasubramanian et al. 2014) (Fig. 1). A fruitful, actively targeted NP system requires a sensitive balance of ligand volume and surface exposure which minimizes immunological response and clearance to give the NPs adequate course time to reach the target cells, while accomplishing suitable binding affinity to the surface receptors expressed on tumor cells. In this aspect the presence of multiple targeting agents per NP surface will yield a binding affinity stronger than for the single ligand, thus enhancing the ligand-receptor binding interaction for the nanoparticles (Zamboni et al. 2012).

Elemental gold (Au) is a dense, soft, malleable, and ductile metal; one ounce (28 g) of gold can be beaten out to 300 square feet. Gold is a good conductor of heat and electricity and is unaffected by air and most reagents. The contemporary use of gold-containing drugs focuses principally on rheumatoid arthritis, with some recent attention to other anti-inflammatory, new anticancer and antimicrobial uses (Pricker 1996). Since antiquated times gold has been considered as the “elixir of life”. It was found with various applications in ancient and medieval era, and has a restorative history in both Eastern and Western conventions. Gold has been known to the Indians since antiquity and nano-formulation, called the ‘*Bhasma*’ (ash) form of gold, has obtained immense therapeutic applications, especially in Sidha

medicine. Trace elements of metallic gold were used for rejuvenation in the Ayurvedic system of medicine, dating back to about 5000 years B.C. (Galib and Prajapati 2011).

Gold nanoparticle (AuNP) with excellent surface plasmon resonance (SPR) characteristics and superior biocompatibility found numerous applications in cancer diagnosis, therapy and many other biomedical fields (Shan and Tenhu 2007; Grzelczak et al. 2008; Sardar et al. 2009; Joseph and Sreelekha 2014). Fluorescent gold nanoclusters (AuNCs) are particular sort of gold nanomaterials with size



Scheme 1 Schematic representation of synthesis and biomedical application of AuNCs. Green synthesis of AuNCs utilizing different reducing and capping agents such as dendrimers, proteins, oligonucleotides and carbohydrates which can be used for biomedical applications such as targeted imaging and drug delivery for cancer

usually less than 3 nm. Not at all like the most prominent and widely understood spherical, large gold nanoparticles, AuNCs do not exhibit surface plasmon resonance (SPR) absorption in the visible region, but have fluorescence in the visible to near-infrared (NIR) region. With focal points of long lifetime, expansive Stokes movement, and biocompatibility, AuNCs have ended up fascinating detecting and imaging materials. AuNCs (Shichibu et al. 2007; Xie et al. 2009; Wei et al. 2011; Mayavan et al. 2011; Guevel et al. 2011; Garcia et al. 2013; Wen et al. 2011; Chen et al. 2013) comprising of several to tens of atoms have drawn greater attention in the recent decade owing to their high fluorescence, good photostability, non-toxicity, excellent biocompatibility and solubility in comparison with other organic fluorophores and semiconducting nanocrystals (Zheng et al. 2007; Lin et al. 2009a; Yang et al. 2011a, b; Shang et al. 2011a). AuNCs having a dimension comparable to the Fermi wavelength of electrons (Zhang and Wang 2014), which place them between single metal atoms and larger NPs (Zheng et al. 2004) enabled size-dependent fluorescence and other attractive features (Chen et al. 1998; Hicks et al. 1999, 2002; Quinn et al. 2003; Qu et al. 2015) making them ideal multi-functional imaging contrast agent. The present chapter mainly focuses on the synthesis strategies of fluorescent AuNCs along with their biomedical applications with special emphasis in oncology (Scheme 1).

2 Mechanisms Behind the Fluorescence of AuNCs

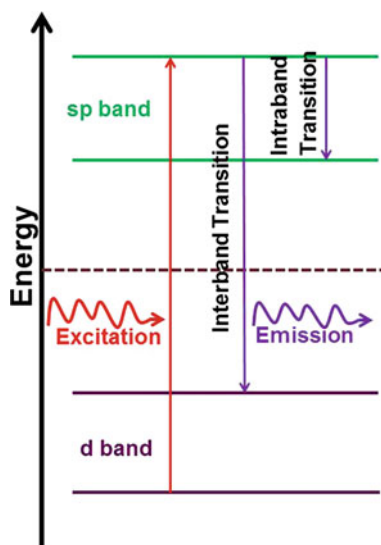
Gold is the most extensively studied inorganic material especially in bio-medical field due to its advisable physical, chemical properties and nontoxicity (Qu et al. 2015). Gold on bulk is highly stable; however nanoscale exhibit size-dependent optical and electronic properties. According to the number of metal atoms, nanoscale metals are roughly classified into three size domains: large NPs, small NPs and clusters, corresponding to three different characteristics length scales respectively (Zheng 2005). In bulk metal, the conduction band has no energy gap separating it from the valence band, so electrons do not suffer from a barrier and are free to move, where the scattering is determined by the electron mean free path. Mostly in case of large and small metal NPs, the size is comparable to or smaller than the electron mean free path, where the motion of electrons becomes limited by the size of the NP and interactions are expected to be mostly with the surface. This feature gives rise to SPR effects (Xu and Suslick 2010) and its optical and electronic behavior is explained by Gustav Mie in 1908 using Maxwell's equations (Mie 1908). In metal NCs, the size of metals is further reduced to around 2 nm or less, down to a few atoms, and the continuous band structure becomes discontinuous and broken up into discrete energy levels, which dramatically changes its optical, electronic and chemical properties compared with metal NPs. Moreover, due to quantum confinement effects of AuNPs with a dimension comparable to Fermi wavelength of electrons, they are too small to support SPR effect (Wu and Jin 2010). NCs are not conductive and plasmonic and cannot be explained using Mie

theory (Alvarez et al. 1997; Schaaff et al. 1997; Hostetler et al. 1998), but Rayleigh scattering principle solved the problem for the NCs because they are having a dimension which is smaller than wavelength of light.

Electronic transitions between the energy levels in fluorescent NCs leads to absorption and emission of light, which enables them to function as potential fluorescent probes in fluorescent bio-sensing and bio-imaging, like quantum dots (QDs) and fluorophores (Li et al. 2014). Although the detailed mechanism for the fluorescence of AuNCs is not completely deciphered yet, the generally accepted model is based on free electron theory. The free electrons on the NCs surface give rise to the polarization in an electronic field and the electron number determines the size dependent fluorescence optics (Haberland 1994; Barnes et al. 2003). Zheng suggested two possible mechanisms to explain the observed emission from this small metal NCs (Zheng 2005), one is due to intra-band (sp/conduction band) transition and the other is inter-band (d-sp) transition (Lin et al. 2009a; Apell et al. 1988) (Fig. 2). The observed fluorescence of AuNCs is determined by the numeric size of the energy level spacing ($E\delta$) (Haberland 1994; Kreibig and Vollmer 1995; Zheng 2007; Chen et al. 2014). When using the thermal energy (ET) as a criterion, AuNCs can emit only when $E\delta$ is much larger than ET where a mobile electron hole can appear and current can flow when $E\delta$ is much smaller than or comparable to ET. Hence AuNCs exhibit stronger fluorescence at low temperature than that at high temperature, mainly because the ET is smaller at a lower temperature. The relationship among the $E\delta$ value of AuNCs and Au atom number (N) and the Fermi energy (E_f) is well predicted by the Jellium model, represented as:

$$E\delta = E_f/N^{1/3}$$

Fig. 2 Possible mechanism of fluorescence of AuNCs by intraband and interband transition. Excitation promotes an electron from the narrow d band to the empty sp band above the Fermi level. Intra-band (sp/conduction band) transition is due to emission above the Fermi level, that is within the conduction band and the inter-band (d-sp) transition is due to the emission probably one near or below the Fermi level



Unique electronic and fluorescent natures are prominent in this nanomaterial (Wilcoxon et al. 1998; Bigoni et al. 2000; Lee et al. 2004; Wang et al. 2005a; Zheng 2007; Bao et al. 2007), generating new horizons of opportunities in imaging.

3 Synthetic Strategies of AuNCs

Recent years witnessed a dramatic increment in publications involving various synthetic strategies adopted for fluorescent AuNCs (Shang et al. 2011a; Qu et al. 2015). AuNCs could be fabricated using different capping agents such as dendrimers, thiols, proteins, oligonucleotides, carbohydrates etc., with various fluorescence quantum yield (QY) (Table 1). Generally, during the synthesis of AuNCs, Au^{3+} is converted to Au^+ and Au in the presence of reducing and capping agents and its entire process depends strongly on the concentration of HAuCl_4 , pH, reaction conditions and many other parameters (Fig. 3). The following section will give a detailed account about the major reducing and capping agents used for the green synthesis of fluorescent AuNCs. Capping agents play a vital role in preventing the NCs from self-aggregation and dissociation. The stability of AuNCs depends mainly on the nature of capping agents used in the fabrication. Various natural and synthetic materials have been widely explored as efficient capping agents.

3.1 Dendrimers

Dendrimers are well-defined, multivalent, monodisperse artificial macromolecules which received continuous attention in recent years as promising candidates for myriad applications especially in cancer therapies and diagnostic imaging. In dendrimers, three dimensional polymers radiate from a central core and are built up by stepwise addition of monomers that contribute to each generation. Presence of internal cavities and high number of functional groups makes them attractive for biological and drug delivery applications.

Dendrimer templated AuNCs exhibited high fluorescence (>10% Quantum Yield) wherein the terminal groups on the dendrimer periphery could be tailored for the further conjugation with affinity ligands. Zheng et al. (2003, 2004) reported synthesis of water soluble, monodisperse, stable fluorescent Au_8NCs using fourth generation poly (amidoamine) (PAMAM) dendrimer and exhibit high QY of 42%. Stable, mono-dispersed and highly crystalline dendrimer-stabilized AuNPs (Au DSNPs) via hydrazine reduction chemistry and stabilized using primary amine-terminated poly (amidoamine) (PAMAM) dendrimers of different generations (generations 2–6) were synthesized with the same molar ratios of dendrimer terminal nitrogen ligands/gold atoms. The size of the synthesized Au DSNPs decreased with the increase of the number of dendrimer generations. These Au

Table 1 Capping agents used for the synthesis of AuNCs

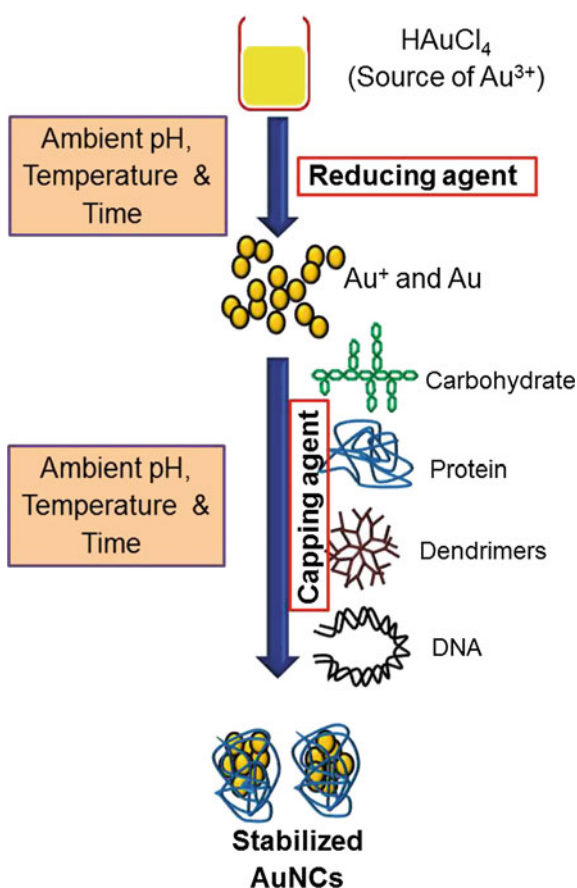
Nature of capping agents	Capping agents	References
Dendrimers	Fourth generation poly(amidoamine) (PAMAM) dendrimer	Zheng et al. (2003, 2004)
	Primary amine-terminated poly(amidoamine) (PAMAM) dendrimers of 2–6 generations	Shi et al. (2006)
Proteins	Dendrimers with terminal amine (G4NH ₂) and hydroxyl (G4OH) groups	Jao et al. (2010)
	Bovine serum albumin(BSA)	Xie et al. (2009)
	Trypsin	Kawasaki et al. (2011b)
	Lysozyme	Wei et al. (2010), Lin and Tseng (2010), Chen and Tseng (2012)
	Transferrin-family proteins	Xavier et al. (2010), Le et al. (2011)
	Horseradish peroxidase (HRP)	Wen et al. (2011)
	DNase I	West et al. (2014)
	RNase A	Kong et al. (2013)
	Isulin	Liu et al. (2011), Garcia et al. (2013)
	Pepsin	Kawasaki et al. (2011a)
Thiols	Substrate peptide 1, CCIHK (Ac), and substrate peptide 3, CCLRRASLG	Wen et al. (2013)
	Tiopronin thiolate	Huang and Murray (2001)
	Glutathione (-SG) and tetraphenyl-porphyrin (H ₂ TPPOASH)	Shibu et al. (2009)
	Multifunctional polymer ligand, containing thiol, thioether, and ester functional groups (PTMP-PVAc)	Huang et al. (2011b)
DNA	Glutathione (reduced)	Ghosh et al. (2012), Roy et al. (2015)
	Poly-cytosine and poly-adenine	Kennedy et al. (2012)
	Single stranded 50-GAGGCGCTGCCYCCACCATGAGC-30, Y = C, A, G, and T	Liu et al. (2012a)
	Hairpin DNAs (HP-DNAs) with a pristine stem segment and cytosine rich loop sequences	Liu et al. (2012b)
Carbohydrate	30 adenosine nucleotides (A ₃₀)	Li et al. (2015a)
	R-, β-, and γ-cyclodextrin (CD)	Shibu and Pradeep (2011)

(continued)

Table 1 (continued)

Nature of capping agents	Capping agents	References
Other molecules	Chitosan and mercaptopropionic acid (MPA)	Sahoo et al. (2014)
	Polyethylenimine (PEI) and NaBH ₂ as reducing agent	Duan and Nie (2007)
	Dimethyl formaldehyde (DMF)	Kawasaki et al. (2010)
	Dihydroliipoic acid	Lin et al. (2009a)
	Amino-terminated poly(1,2-butadiene)	Yabu (2011)

Fig. 3 Schematic representation of synthesis of AuNCs. During the synthesis of AuNCs, Au³⁺ in HAuCl₄ is converted to Au⁺ and Au in the presence of reducing and capping agents such as dendrimers, proteins, oligonucleotides, carbohydrates and it entire process depends strongly on the concentration of HAuCl₄, pH, temperature, reaction time etc



DSNPs are fluorescent and displayed strong blue emission intensity at 458 nm and could be further modified with various biological ligands for the application in biosensing and targeted cancer therapeutics (Shi et al. 2006). Jao et al. (2010)

employed a specific ion-pair approach using the dendrimers with terminal amine (G_4NH_2) and hydroxyl (G_4OH) groups for trapping gold salts. This facile strategy not only led to the polarity-dependent strong ion-pair association ($AuCl_4/G_4NH_2$ pair and $AuBr_4/G_4OH$ pair) but also significantly enhances the QY of gold nanodots from 20 to 62% after microwave irradiation.

3.2 Proteins

Bio-mineralization is a natural process in which biological organism's intake metal species to subsequently form mineral structures. Inspired by this process nanostructures could be formed by harnessing the biological organisms or macromolecules ability to naturally intake and arrange inorganic materials (Fendler 1997; Bhattacharya and Gupta 2005; Crookes-Goodson et al. 2008; Chen and Rosi 2010; Chevrier et al. 2012). Green chemistry approaches using biological materials was widely exploited in stabilizing gold atoms producing stable fluorescent AuNCs with excellent biocompatibility, which renders them suitable for biomedical applications. Proteins are the major bio-macromolecules exploited in green chemistry approach due to their numerous physical and chemical assets. Xie et al. (2009) developed highly fluorescent red emitting protein stabilized AuNCs by common protein bovine serum albumin (BSA) (Fig. 4A, B(a)). Besides being highly stable both in solutions (aqueous or buffer) and in the solid form, the light emitting AuNCs consist of 25 gold atoms (Au_{25}). Motivated with this promising approach, many other synthetic procedures were developed using other proteins such as trypsin (Kawasaki et al. 2011b), lysozyme (Wei et al. 2010; Lin and Tseng 2010; Chen and Tseng 2012), transferrin-family proteins (Xavier et al. 2010; Le et al. 2011), horseradish peroxidase (HRP) (Wen et al. 2011), DNase 1 (West et al. 2014), RNase A (Kong et al. 2013), insulin (Liu et al. 2011; Garcia et al. 2013) and much more.

Kawasaki et al. (2011a) reported the pH-dependent synthesis of pepsin-mediated AuNCs with fluorescent emissions of blue, green and red from Au_5 (Au_8), Au_{13} , and Au_{25} , respectively. The different charges on the pepsin molecule at different pH values could affect the structural nature and the strength of interaction between the pepsin chains and the gold surface or gold ions, leading to the formation of AuNCs with different sizes. Preparation of AuNCs for the detection of protein modifying enzymes and their inhibitors using peptides found widespread attention. Designed substrate peptides such as substrate peptide 1, CCIHK (Ac), and substrate peptide 3, CCLRRASLG were used for the synthesis of AuNCs and studied the effect of enzymatic modifications on their luminescence using two appropriate PTM enzymes, histone deacetylase 1 (HDAC 1) and protein kinase A (PKA) respectively. The study revealed that AuNCs fluorescence can be dynamically decreased with increasing concentration of enzymes, which offer label-free biosensor platform for the detection of PTM enzymes (Wen et al. 2013).

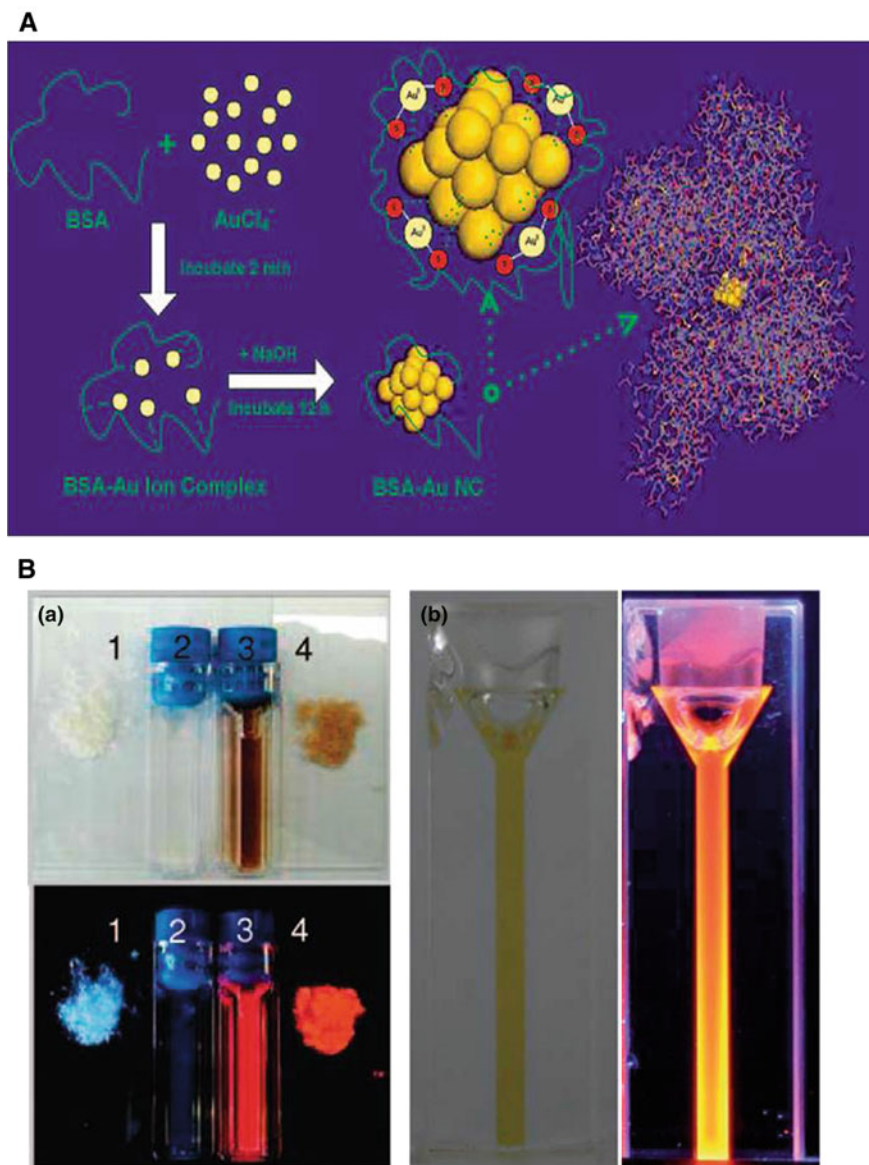


Fig. 4 **A** Schematic representation of the formation of AuNCs in BSA Solution. **B(a)** Photographs of BSA (1) powder and (2) aqueous solution, and BSA-AuNCs (3) aqueous solution and (4) powder under (top) visible and (bottom) UV light (Reprinted with permission from Xie et al. (2009) © 2009 American Chemical Society). **(b)** Photographs of aqueous solution of DPA-AuNCs in room light and under a UV light source with wavelength 365 nm respectively (Reproduced from Shang et al. (2011) with permission of The Royal Society of Chemistry)

Enzymes are widely employed as reducing and capping agent in preparation of AuNCs. The lysozyme-stabilized gold fluorescent clusters (LsGFC) with an average size of 1 nm and emission at 657 nm were effectively synthesized (Wei et al. 2010). Photo stable, trypsin-capped fluorescent AuNCs with an average size of 1 nm and a red emission at 645 nm were reported for the sensitive and selective detection of Hg^{2+} ions (Kawasaki et al. 2011b). Similarly construction of horseradish peroxidase (HRP) functionalized fluorescent AuNCs (HRP-AuNCs) via a bio-mineralization process at physiological conditions for the detection of hydrogen peroxide was also attempted. The fluorescence of HRP-AuNCs can be quenched quantitatively by adding H_2O_2 , indicating that HRP enzyme remains active and enables catalytic reaction (Wen et al. 2011). The enzyme DNase 1 stabilized AuNCs (DNase 1: AuNCs) with core size consisting of either 8 or 25 atoms exhibited blue and red fluorescence respectively. In addition to the intense fluorescence emission, the synthesized DNase 1: AuNCs hybrid retained the native functionality of the protein, allowing simultaneous detection and digestion of DNA with a detection limit of 2 $\mu\text{g}/\text{ml}$, hence could be conveniently employed as efficient and fast sensors to augment the current time-consuming DNA contamination analysis techniques (West et al. 2014). Synthesis of AuNCs by core etching of AuNPs using appropriate ligands (Muhammed et al. 2008; Lin et al. 2009a; Qian et al. 2009) also attained scientific attention. Muhammed et al. (2010) employed synthesis of a luminescent AuNCs by core etching of mercaptosuccinic acid protected AuNPs using BSA(AuQC@BSA). The cluster core contains Au_{38} and exhibit QY of $\sim 4\%$. This AuQC@BSA is exploited as a “turn-off” sensor for Cu^{2+} ions and a “turn-on” sensor for glutathione detection.

Few of the amino acids play a key role in protein and peptide templated AuNCs synthesis due to their reducing and capping efficiency with gold (Brown et al. 2000; Naik et al. 2004). Tan et al. (2010) analyzed all the 20 amino acids alone and in combinations to determine their capability as a template in AuNCs preparation. Tryptophan was identified for being the strongest reducing agent and was therefore interdigitated into custom peptides for its reducing property. In a similar fashion; histidine was selected as the strongest metal binding amino acid and was also interdigitated into another set of peptides. From these preliminary peptide results, more diverse combinations with other amino acids were also investigated to determine the resultant shape and size of the AuNPs, along with tracking the periods of reaction initiation, growth, and termination (Chevrier et al. 2012). Tyrosine residues can reduce Au (III) or Ag (I) ions through their phenolic groups; their reduction capability can be greatly improved by adjusting the reaction pH above the pKa of Tyr (~ 10) (Xie et al. 2007). The AuNCs formed in the BSA solution could have been stabilized by a combination of Au-S bonding with the protein (via the 35 Cys residues in BSA), and the steric protection due to the bulkiness of the protein (Xie et al. 2009). Yang et al. (2011b) reported the synthesis of water-soluble, mono-dispersed and bluish green-emitting Au_{10} NCs through a simple reaction, in which histidine served as both reducing and protecting or capping ligand. The mechanism of this proposed reaction was explored and the

reducing ability of histidine was proved to be attained from its prominent imidazole group.

One-pot synthesis of fluorescent AuNCs templated with L-tyrosine which serves both as a reducing and capping agent (AuNCs@Tyr) were employed for investigating tyrosinase (TR) activity on the basis of aggregations of AuNCs@Tyr on its active sites during the catalysis reactions, thus leading to the fluorescence quenching of AuNCs@Tyr. The as prepared AuNCs@Tyr exhibited a fluorescence emission at 470 nm with a QY of approximately 2.5%. Significantly, TR has been considered as a critical marker for melanoma owing to its specific expression in melanoma cells. Therefore, this analytical method towards investigating TR activity may have broadened avenues for meaningful clinical applications (Yang et al. 2014).

3.3 Thiols

Thiols are the class of organic compounds that contain a sulfhydryl group (-SH), also known as a thiol group, that is composed of a sulfur atom and a hydrogen atom attached to a carbon atom (Prakash et al. 2009). Thiols containing small molecules are extensively used to stabilize AuNCs mainly because they can form strong Au-S bonding with Au atoms or ions (Link et al. 2002; Chen et al. 2014; Qu et al. 2015). Huang and Murray (2001) reported water soluble, monolayer protected gold clusters (MPCs) using tiopronin thiolate with an excitation and emission at 451 nm and 700-800 nm respectively. Fluorescent, Au₂₂ clusters (Au₂₂[(-SG)₁₅(-SAOPPTH₂)₂]) starting from Au₂₅ clusters protected with glutathione (-SG) by a combined core reduction/ligand exchange protocol using tetraphenyl-porphyrin (H₂TPPOASH) were effectively prepared. The absence of a 672 nm intra-band transition of Au₂₅ and the simultaneous emergence of new characteristic peaks at 520 and 635 nm in UV-visible spectrum indicated the formation of the Au₂₂ core (Shibu et al. 2009).

Stable, blue fluorescent AuNCs of size and QY ~ 1.2 nm and 24.3% respectively using a multifunctional polymer ligand, containing thiol, thio-ether, and ester functional groups (PTMP-PVAc) were fabricated by adjusting the molecular weight and concentration of the polymer ligand (Huang et al. 2011b). Similarly near-infrared (NIR) luminescent AuNPs (NIRL-AuNPs) by heat-assisted reduction of a gold(I)-thiol complex was prepared which exhibited strong emission with peak maximum at 810 nm, large stokes shifts (>400 nm) and stabilities towards photo-bleaching and chemical oxidation (Tu et al. 2011). Luminescent and water-soluble AuNCs (Au18SG14) were prepared using glutathione by a slow reduction process which emits red light in both aqueous and solid state under UV illumination but with a QY of only 0.053%. Although thiol protected AuNCs proved to be of great promise, the main problem behind them is the relatively low (0.001–0.1%) yield (Ghosh et al. 2012). Roy et al. (2015) successfully exploited the synthesis of blue, green, orange-red, red and NIR emitting AuNCs in aqueous media by using

a bioactive peptide glutathione (reduced) at physiological pH with excellent stability. Matrix-assisted laser desorption ionization-time-of-flight mass spectrometry (MALDI-TOF MS) analyses showed that the core structure size of the five different gold clusters are Au₇ (blue), Au₁₆ (green), Au₁₉ (orange-red), Au₂₁ (red) and Au₂₂ (NIR). The AuNCs demonstrated better cell internalization and non-toxicity on human lung adenocarcinoma A549 cells.

3.4 DNA

After water and oxygen, DNA is likely the most celebrated particle of life known to human race. This is not astounding, as we as a whole realize that an eye-catching, double helical particle of DNA conveys guidelines to produce and gather every one of the segments of a living being. The abundance of data encoded in a DNA molecule regularly eclipses its unique physical, chemical and biological properties (Maffeo et al. 2014). DNA has the unique capabilities to build complex nanostructures via self-assembly, which results from hydrogen-bonds formation between base pairs and hydrophilic-hydrophobic interactions (La Bean and Li 2007). The use of DNA as a template for metal NCs synthesis attained greater momentum due to the biocompatibility and extensive biomedical applications that the biomolecule holds. The mechanism of bonding between AuNPs and DNA and the factors which control its efficiency was well studied and documented (Kryachko and Remade 2005a, b; Shukla et al. 2009), which demonstrated the involvement of two major bonding factors: the anchoring, either of the Au-N or Au-O type, and the non-conventional N-H-Au hydrogen bonding. Shukla et al. (2009) revealed the interaction of AuNCs (Au_n, Where n = 2, 4, 6, 8, 10, 12) with nucleic acid purine base guanine (G) and the Watson-Crick guanine-cytosine (GC) base pair through the major groove site (N7 site of guanine) of DNA by theoretical means (density functional theory (DFT)) and observed a greater interaction of AuNCs with the GC pair than with isolated guanine. Blue fluorescent AuNCs were prepared in the presence of poly-cytosine DNAs at low pH and poly-adenine at neutral pH using citrate as the reducing agent (Kennedy et al. 2012). Similarly stable, water-soluble and red-emitting AuNCs serving as promising nanoprobe in bio imaging and related fields were fabricated using single stranded DNA (50-GAGGCGCTGCCY CCACCATGAGC-30, Y = C, A, G, and T) and dimethylamine borane as a mild reductant in acidic solution (Liu et al. 2012a).

Liu et al. (2012b) compared sequence-dependent formation of fluorescent AuNCs using hairpin DNAs (HP-DNAs) with a pristine stem segment and varied loop sequences and observed that the emission behavior of the HP-DNA hosted AuNCs is dependent on the loop sequences. It was documented that the most efficient host to produce fluorescent AuNCs is the cytosine loop compared with other nucleotide's loops and the emission behavior of AuNCs hosted by the single-stranded DNAs (ss-DNAs) with an identical base composition to the corresponding HP-DNAs still exhibits a cytosine-rich dependence. A UV-light assisted

method for the synthesis of AuNCs using repeats of 30 adenosine nucleotides (A₃₀) was reported, which could be used for the detection of specific nucleic acid targets in human serum via the formulation of clusters along with the SYBR Green 1 that specifically binds to DNA sequence. The so formed AuNCs exhibited moderate fluorescence at 475 nm while on binding with perfectly matched nucleotide sequences, emit fluorescence at 525 nm that paved the way for the development of beneficial metal NCs in both research and medicine (Li et al. 2015b).

3.5 Carbohydrates

Carbohydrates are one of the most utilized classes of biological macromolecules for bio medical applications. They can differ significantly in size ranging from monosaccharides to polysaccharides consisting of many thousands of carbohydrate units. One of the most significant features of carbohydrates is their ability to form branched molecules, which stands in contrast to the linear nature of DNA, RNA, and proteins. Combined with the large heterogeneity of the monosaccharides, they exhibit a significantly higher structural diversity than other abundant macromolecules which makes them suitable candidates with ease of structural modification and manipulation in NP synthesis and modification (Frank and Schloissnig 2010). Carbohydrates have been widely used as both reducing and capping agents in the synthesis of AuNPs (Katti et al. 2009; Shervani and Yamaoto 2011; Thygesen and Jensen 2015) and attracted scientific attention due to its non-toxic and biocompatible nature. A simple and versatile methodology was adopted for tailoring sugar-functionalized fluorescent glyco-nanoparticles using biologically significant oligosaccharides as well as with differing carbohydrate density. The resultant nanoclusters are water soluble, stable and their highly polyvalent network can mimic glyco-sphingolipid clustering and interactions at the plasma membrane, providing a controlled system for glycobiological studies (Thygesen and Jensen 2015). Au₁₅ quantum clusters anchored to R-, β-, and γ-cyclodextrin (CD) cavities was prepared, which are intensely luminescent in liquid as well as in solid state. Moreover, evaporation of the cluster solutions leads to luminescent gel like materials (Shibu and Pradeep 2011). Sahoo et al. (2014) synthesized AuNCs using chitosan and mercaptopropionic acid (MPA) and embedded as chitosan nanoparticles which exhibited simultaneous red, green, and blue emission on exposure to light of varying wavelength. The as formed AuNCs were conjugated to pCD-UPRT suicide gene that on targeting tumor cells caused apoptosis and helped in imaging.

3.6 Other Materials

Apart from the above mentioned molecules many other materials are also employed in the preparation of fluorescent AuNCs. A ligand-induced etching process was employed

in which hyper branched and multivalent coordinating polymers such as polyethylenimine (PEI) react with preformed gold nanocrystals to form atomic AuNCs which are soluble in water with an excitation and emission maxima located at 421 and 505 nm, respectively. These small atomic clusters consist of only 8 gold atoms (Au_8) and upon treatment by strong reducing agent such as NaBH_4 , their excitation and emission peaks were shifted to 353 and 445 nm respectively (Duan and Nie 2007). Kawaski et al. (2010) reported the synthetic strategy for obtaining DMF protected AuNCs with high thermal stability ($\sim 150^\circ\text{C}$) and dispersion stability in various solvents and having less than 20 gold atoms including Au_8 and Au_{13} . Water soluble dihydrolipoic acid stabilized AuNCs (AuNC@DHLA) were prepared which emits fluorescence upon ligand exchange with dihydrolipoic acid and also demonstrated tumor specific internalization in human hepatoma HepG₂ cells (Lin et al. 2009b). Blue light-emitting AuNCs were obtained by a simple one-pot process via reflux of Au ions with amino-terminated poly (1,2-butadiene) in toluene (Yabu 2011). A facile strategy for the preparation of water-soluble, fluorescent AuNCs using a mild reductant, tetrakis(hydroxymethyl)phosphonium chloride (THPC) and capped by zwitterionic functional ligand, D-penicillamine (DPA) was recently reported (Fig. 4B(b)). These DPA-AuNCs displayed excitation and emission bands at 400 and 610 nm, respectively with a fluorescence QY of 1.3% and demonstrated internalization in human cervical carcinoma HeLa cells (Shang et al. 2011b).

4 Bio-medical Applications of AuNCs

4.1 *Bio Imaging and Targeted Therapy*

Biomedical imaging techniques have accelerated the efficient early cancer detection and in treatment monitoring. Unfortunately, many of the conventional biomedical imaging techniques have lesser sensitivity to detect tumors when they are less than a centimeter in diameter. Efficient molecular imaging techniques with targeting moieties conjugated imaging agents can monitor biological processes at the cellular and subcellular levels with high sensitivity and specificity. NP-based molecular imaging agents can overcome biological barriers inside the body which leads to the development of multifunctional NPs for the simultaneous targeting, imaging and therapy of cancer (Sivasubramanian et al. 2014). Optical imaging techniques have wider applications due to its advantages such as low cost, low-energy radiation, high sensitivity, real-time monitoring and non-invasive or minimally invasive testing (Zheng et al. 2012). Multifunctional NPs based on AuNCs produced with green chemistry approaches are promising optical fluorescent probes for combined targeting, imaging and delivery of chemotherapeutics because of their biocompatibility, large stoke shift, long lifetime, photo and chemical stability and ease in conjugation (Fig. 5).

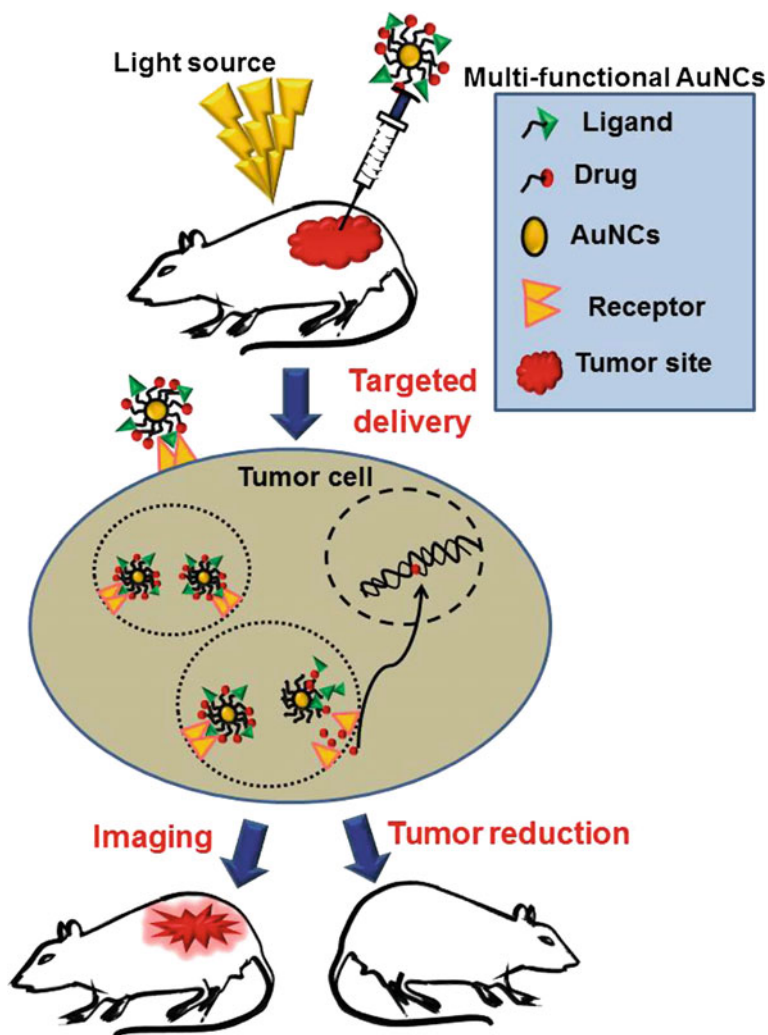


Fig. 5 Schematic diagram representing the mode of action of AuNCs in vivo. The ligand conjugated AuNCs with chemotherapeutics targeted specifically to the cancerous cell surface receptor after injection. This leads to internalization of Au NCs with drugs by receptor mediated endocytosis. Inside the tumor cells, the AuNCs release drugs and also help imaging. Chemotherapeutic drugs such as doxorubicin (Dox) and cisplatin enter the nucleus, resulting in cell death

Polavarapu et al. (2011) investigated one and two photon excitation and emission properties of water soluble glutathione monolayer protected AuNCs. The two-photon absorption cross section of these AuNCs was calculated through z-scan method using a mode-locked Ti:sapphire oscillator seeded regenerative amplifier and found to be 189,740 GM which is much higher compared with the values reported for

organic fluorescent dyes and quantum dots which make them a promising alternative for one- and two-photon bio-imaging and other nonlinear optical applications. Biological labeling and tumor targeted therapy could be achieved using AuNCs decorated with biomarker molecules on the surface (Huang et al. 2009, 2011a). The biomarkers could be tumor specific ligands such as small molecules, peptides, proteins, monoclonal antibodies and so forth which are specific for cell surface receptors over expressed on cancer cells as compared to normal cell (Table 2). Commonly used methods for bio-conjugation is through 1-[(3-dimethylamino)-propyl]-3-ethylcarbodiimide hydrochloride (EDC) and sulfo-N-hydroxysuccinimide (sulfo-NHS) activation in which NCs with functional groups such as primary amide or carboxylic acid can conjugate with other carboxylic or amino-terminal biomolecules. Avidin molecule containing NH_2 group can be conjugated to the carboxylic acid group containing capping agent of the AuNCs through EDC/NHS chemistry to synthesize AuNCs with high affinity to biotin overexpressed cancer cells. Likewise folic acid (FA) conjugated AuNCs can be internalized by certain cancerous cells, such as ovarian, oral, and breast which are rich in FA receptors (FR).

Wang et al. (2011a) investigated biocompatible AuNCs for in vitro and in vivo tracking of human aortic endothelial cells (HAEC) and endothelial progenitor cells (EPC) by delivering via the liposome complex and found no impaired angiogenesis by tube formation assay. In in vivo study using hind limb ischemic mice, intramuscular injection of AuNCs labeled human EPC showed that the cells preserved an angiogenic potential and exhibited traceable signals after 21 days which

Table 2 Ligands conjugated AuNCs and its targeting moieties

AuNCs	Ligand	Target	References
Glutathione thiolate capped Au25SG18	Streptavidin	Biotin	Muhammed et al. (2009)
Dihydrolipoic acid (DHLA) capped AuNCs (AuNC@DHLA)	Streptavidin	Biotin	Lin et al. (2009a)
BSA capped AuNCs	Folic acid	Folic acid receptor	Muhammed et al. (2010), Lin et al. (2013a)
Ovalbumin capped AuNCs	Folic acid	Folic acid receptor	Qiao et al. (2013)
Silica coated AuNCs (AuNCs@SiO ₂)	Folic acid	Folic acid receptor	Zhou et al. (2013)
BSA capped AuNCs	Monoclonal antibody against CD33	CD33	Retnakumari et al. (2011)
11-mercaptoundecanoic acid capped AuNCs	TAT-peptide	Nucleus	Vankayala et al. (2015)
BSA capped AuNCs	Herceptin	ErbB-2	Wang et al. (2011b)

highlighted the promising biocompatibility of this fluorescent probe. Physiological changes in cellular pH are better indicators of disease initiation or progression. Therefore, a pH-responsive material often serves as excellent tools in the fundamental understanding of cell biology or medicine for disease diagnosis and therapy. Negatively charged AuNCs synthesized using glutathione and cysteamine as surface ligands, exhibited high resistance to non-specific protein adsorption and strong pH-dependent adsorption in live cell membranes of HeLa cells within a biological pH range (5.3–7.4). Thus, metal NCs with pH-dependent membrane adsorption might find new applications in tumor diagnosis and therapy (Yu et al. 2011). Shang et al. (2011b) demonstrated the application of DPA–AuNCs as fluorescent nanoprobe in bioimaging of HeLa cells using zwitterionic functional ligand, D-penicillamine (DPA), as a capping agent (Fig. 6a). DPA–AuNCs was used for targeted biological imaging applications because the carboxylic and amino groups of DPA allow further functional molecules to be conjugated to the AuNCs for specific tagging. Established simple and spontaneous procedure for the synthesis of fluorescent AuNCs by cancerous cells such as HepG2 and K562 was developed in which the AuNCs is formed by Au(III) reduction inside the cellular cytoplasm and ultimately concentrate around their nucleoli, thus affording precise cell imaging and this does not occur in non-cancerous cells, as evidenced with L02 cells used as controls (Fig. 6b) (Wang et al. 2013).

Bright-red-emitting sub-nanocluster, Au₂₃, prepared by the core etching of glutathione thiolate capped Au₂₅SG18 was used for imaging the hepatocellular carcinoma cell line HepG2 by employing the avidin–biotin interaction. Biotin is a water-soluble B-complex vitamin that is a cofactor in the metabolism of fatty acids and is present in large volume in these cancerous cells. For the specific labeling of the cells, Au₂₃ clusters were functionalized with streptavidin following an EDC coupling reaction. Since biotin strongly binds with streptavidin, the cells can be imaged using the fluorescence of the clusters (Muhammed et al. 2009). In a similar study, dihydrolipoic acid (DHLA) capped AuNCs (AuNC@DHLA) particles with the quantum yield of around 13% were conjugated to biologically relevant molecules such as PEG, BSA, avidin and streptavidin by EDC chemistry separately to compare the cellular internalization in HepG2 cells. Streptavidin-conjugated AuNCs stained the biotin containing cells with high intensity which highlights the fact that streptavidin-conjugated AuNC@DHLA can specifically label endogenous biotin (Lin et al. 2009b). BSA capped AuNCs (AuQC@BSA) functionalized with FA (folic acid) following EDC coupling of FA and BSA exhibited FR targeted cellular uptake in cancer cells. Cancerous cells are employed with increased FRs when compared to normal cells, and therefore FA-conjugated AuQC@BSA could be used for specific detection of cancer cells (Tan et al. 2010). Lin et al. (2013b) employed FR targeted internalization of BSA–Au–FA nanocomplex on human gastric carcinoma MGC803 cells. In a similar study ovalbumin protected AuNCs with FA as the targeting ligand linked by homopolymer N-acryloxysuccinimide has been investigated and its internalization was demonstrated on HeLa cells (Qiao et al. 2013).

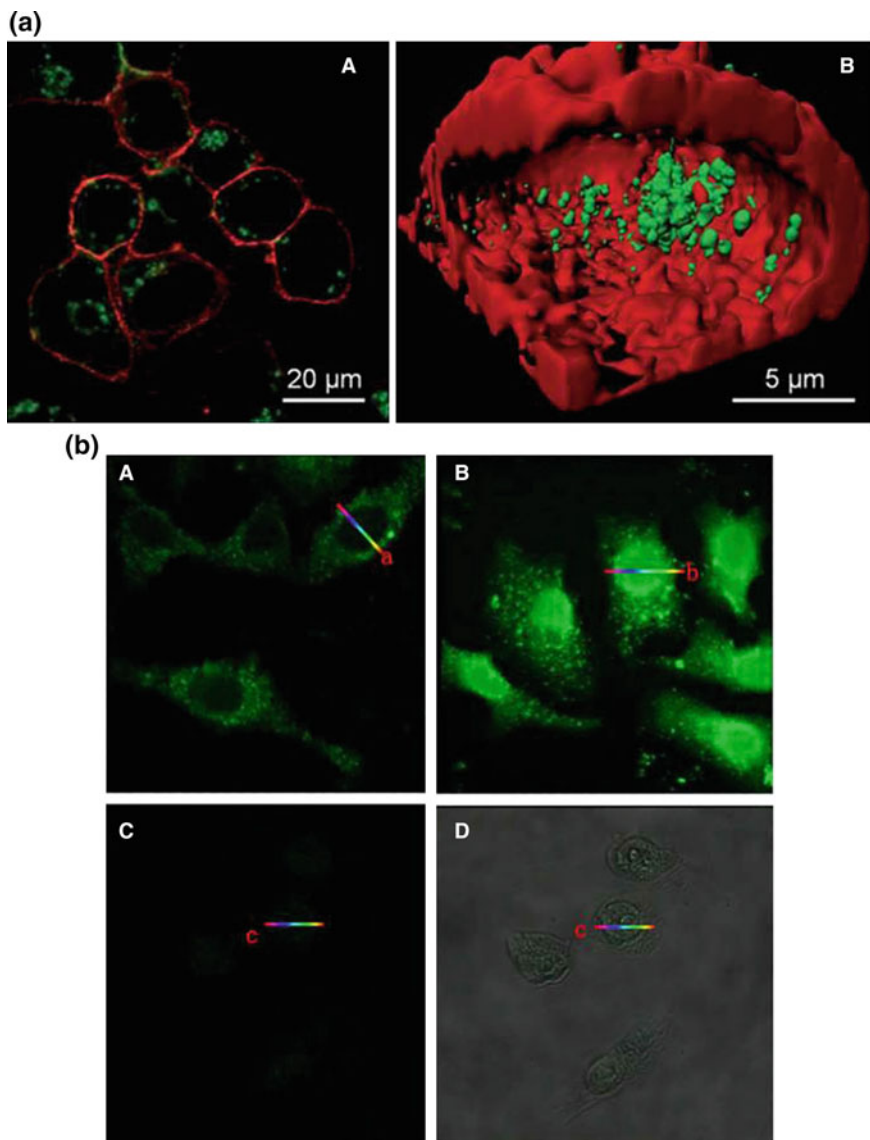


Fig. 6 **a** Internalization of DPA-AuNCs in HeLa cells. **A** Confocal image after 2 h incubation with DPA-AuNCs. **B** Cross-section of a 3D image reconstruction. Membranes were stained with the red dye DiI. Images were taken by 2-photon excitation at 810 nm. DPA-AuNCs (Reproduced from Shang et al. (2011b) with permission of The Royal Society of Chemistry). **b** Laser confocal fluorescence micrographs of HepG2 (**A** and **B**) and L02 control cells (**C** and **D**) incubated with identical 10 mmol/L HAuCl₄ solutions. **A** after 24 h incubation; **B**, **C** and **D** after 48 h incubation; **D** Overlay of the morphological and fluorescence image of **C**. Images were acquired at 400-fold magnification (Reprinted by permission from Macmillan Publishers Ltd: Scientific Reports (Wang et al. 2013), © 2013)

Molecular receptor (CD 33) targeted flow cytometry based detection and imaging of cancer cells was employed using monoclonal antibody conjugated BSA-AuNCs. The protein protected clusters were conjugated with monoclonal antibody against CD33 myeloid antigen, which is overexpressed in the primitive population of acute myeloid leukemia (AML) cells. The as prepared AuNC-CD33 conjugates having average size of ~ 12 nm retained bright fluorescence with excellent biocompatibility. Target specificity of the conjugates for detecting CD33 expressing AML cells in flow cytometry displayed specific staining of $\sim 95.4\%$ of leukemia cells within 1–2 h compared to a non-specific uptake of $\sim 8.2\%$ in normal human peripheral blood cells which was further confirmed with confocal imaging (Retnakumari et al. 2011). The possibility of using BSA capped ultra-small NIR emitting AuNCs as contrast imaging agents for tumor fluorescence imaging in vivo was explored and demonstrated by subcutaneous, intramuscular and intravenous injection in mice model (Fig. 7a). The fluorescence imaging signal of the tail vein administrated AuNCs in living organisms can spectrally be well distinguished from the background with maximum emission wavelength at about 710 nm, and the longer circulation time of AuNCs up to 5 h and clearance within 24 h promises continuous imaging in vivo. Moreover, the uptake of AuNCs by the reticulo-endothelial system is relatively low because of its ultra-small hydrodynamic size (~ 2.7 nm) and the body weights of mice injected with AuNCs had only changed slightly after 4 weeks compared with control mice, indicated that the ultrasmall NIR AuNCs had no potential toxicity to the animal model. The NCs also displayed tumor accumulation in MDA-MB-45 and HeLa tumor xenograft models due to the EPR effects which promotes its promising application as contrast imaging agents for in vivo fluorescence tumor imaging (Fig. 7b) (Wu et al. 2010).

Nucleus targeting using AuNCs was designed by conjugating nucleus targeting trans-activating transcriptional activator (TAT) peptide with AuNCs to perform simultaneous in vitro and in vivo fluorescence imaging, gene delivery and NIR light activated photodynamic therapy for effective cancer cell killing. The TAT peptide–Au NCs exhibit excellent photo-stabilities, and appreciable biocompatibility in HeLa cells as well as in vivo zebrafish model system. They demonstrated the co-localization and distribution in the cytoplasm with a significant fraction ($>50\%$) entering into the nucleus of HeLa cells which could also serve as DNA delivery cargoes with ultrahigh cellular uptake ($\approx 90\%$) and gene transfection efficiencies ($\approx 80\%$) compared to commonly adopted LP2000 liposome gene carrier in HeLa cells. Moreover, the TAT peptide–AuNCs also sensitizes the formation of singlet oxygen upon long NIR light (850–1100 nm) excitation enabling effective photodynamic therapeutic effects on destruction of cancer cells via photo-induced DNA damages (Vankayala et al. 2015). Methionine was covalently linked to BSA stabilized AuNCs by EDC chemistry for tumor-selective optical imaging of methionine-dependent malignant cells. Hydrophilic indocyanine green (ICG) derivative MPA, a NIR fluorescent dye, was used to label methionine-modified AuNCs (Au-Met-MPA) for NIR tumor imaging which displayed non-toxicity and tumor specific bio-distribution pattern in different

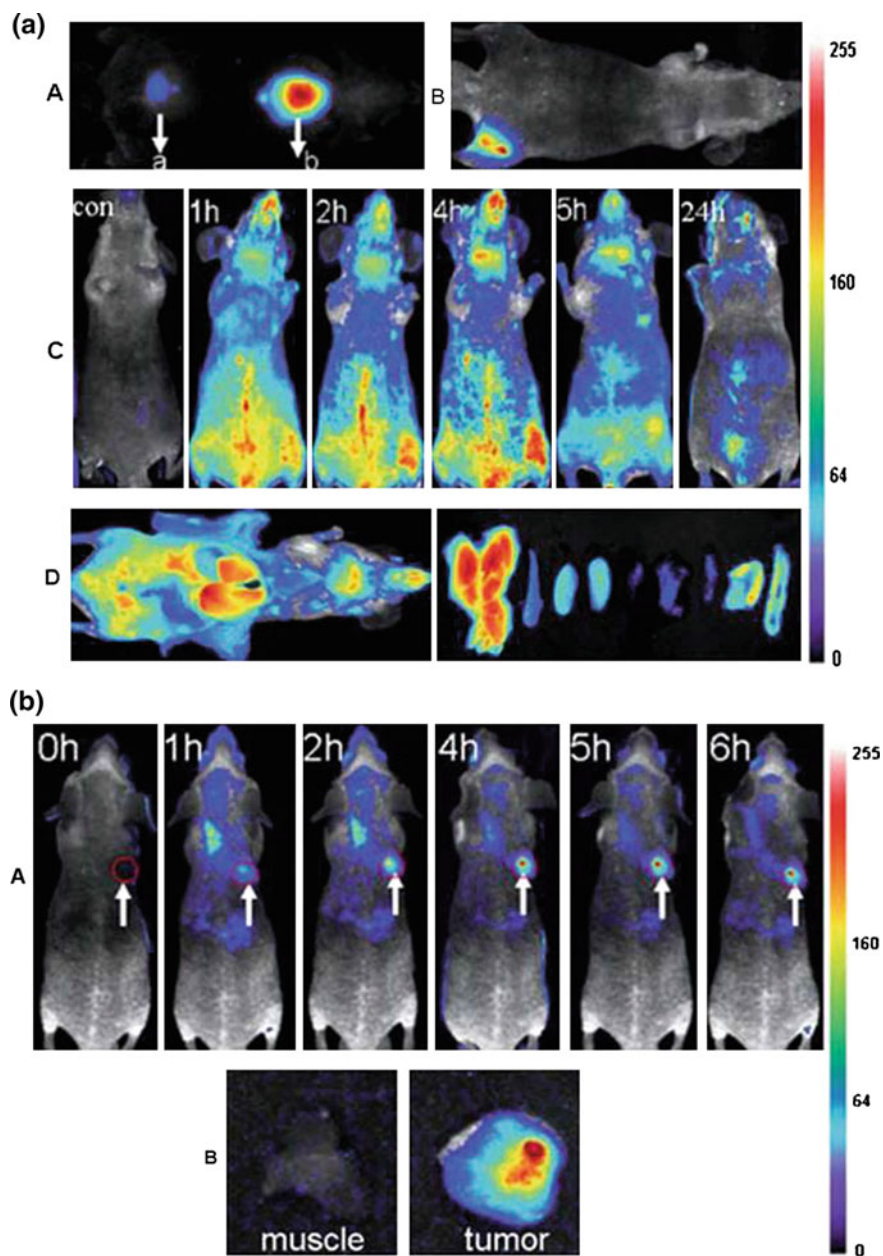


Fig. 7 a BSA-AuNCs as contrast imaging agents for tumor fluorescence imaging in vivo was demonstrated by subcutaneous *A*, intramuscular *B* and intravenous *C* injection in mice model at different time points of post injection. *D* Ex vivo optical imaging of anatomized mice and some dissected organs such as liver, spleen, left kidney, right kidney, heart, lung, muscle, skin and intestine from *left to right*. **b** Tumor accumulation BSA-AuNCs in MDA-MB-45 tumor xenograft models due to the EPR effects (Reproduced from Wu et al. (2010) with permission of The Royal Society of Chemistry)

tumor bearing mouse models. Doxorubicin (DOX), a widely used clinical anti-cancer drug, was immobilized on the methionine modified AuNCs to form a pro-drug, Au-Met-DOX. The enhanced tumor affinity and improved anti-tumor activity of this pro-drug were demonstrated on mouse sarcoma S180 tumor bearing mice. All the results in this study lead to tumor-targeted imaging and therapeutic efficacy of AuNCs as a core for the design of pro-drug in the field of cancer therapy (Chen et al. 2012). A fluorescence enzyme mimetic nanoprobe based on FR targeting AuNCs used for tumor tissues visualization was fabricated by one-step incubation method. The nanoprobe could distinguish efficiently cancerous cells from normal and could be a potential diagnostic tool for cancer imaging and prediction (Hu et al. 2014).

Recently, facile Au/Ce nanoclusters were synthesized by doping trivalent cerium ion into seed crystal growth process of gold and stabilized by glutathione which could be used as an excellent fluorescent probe for marking tumor cells due to their targeted absorption. These nanoclusters had no obvious cell cytotoxicity effect on HeLa, HepG2 and L02 cells and demonstrated in vivo imaging efficiency on a xenograft tumor model of cervical carcinoma (Ge et al. 2015). Since AuNCs can preferentially accumulate in tumor via the improved EPR effect due to its ultra-small size, they found profound applications as radio-sensitizers for cancer radiotherapy (Zhang et al. 2013). In an interesting study, fluorescent BSA-protected AuNCs conjugated with Herceptin (AuNCs-Her), for specific targeting and nuclear localization in ErbB-2 over-expressing breast cancer cells and tumor tissue for simultaneous imaging and cancer therapy was successfully prepared. These AuNCs-Her could escape the endo-lysosomal pathway and enter the nucleus of cancer cells and enhances the anticancer therapeutic efficacy of Herceptin by the induction of DNA damage which was evidenced in human breast cancer SK-BR3 cells (Wang et al. 2011b). In a separate work, folic acid conjugated silica coated AuNCs (AuNCs@SiO₂) were developed for targeted dual-modal fluorescent and X-ray computed tomography imaging (CT) of gastric cancer cells with over expression of FR. Tail vein injection of the AuNCs@SiO₂-FA in MGC803 nude mice models exhibited excellent red emitting fluorescence optical property and X-ray absorbance for optical and CT dual-modality imaging (Zhou et al. 2013).

4.2 Sensing Applications

Fluorescent AuNCs found tremendous applications as sensors in the detection of metal ions, small molecules and biological macromolecules due to its quenching or enhancing effect when Au⁺ ions interacting with them. The impact of these AuNCs on resolving the headed issues in environment as well as medical sciences can provide greater tool for early detection of minuscule concentration of organic and inorganic molecules. In this context a discussion about the possible applications of as metal ion sensors, biosensors and so on need special attention.

4.2.1 Metal Ion Sensors

Presence of heavy metal ions such as Hg^{2+} , Cd^{2+} , Pb^{2+} and Cu^{2+} cause hazardous health issues because of their property of binding with vital organs or cellular components (Wei et al. 2010; Lin et al. 2010; Wang et al. 2014; Ding et al. 2014). Routine detection of mercuric ions (Hg^{2+}) is central to environmental monitoring in aquatic ecosystems. The first report in which the fluorescence of alkane thiols capped AuNCs (11-MUA-AuNPs) was quenched by the presence of mercury (II) (Hg^{2+}) due to Hg^{2+} -induced aggregation of AuNCs (Huang et al. 2007a) provide a ray of hope for enabling heavy metal detection using AuNCs. Similarly, Xie et al. (2010) developed a simple paper test strip system for the rapid routine monitoring of Hg^{2+} ions using AuNCs. Lysozyme type VI-stabilized gold nanoclusters (Lys VI-AuNCs) as a probe for the ultrasensitive detection of Hg^{2+} and CH_3Hg^+ in seawater based on fluorescence quenching due to the interaction between $\text{Hg}^{2+}/\text{CH}_3\text{Hg}^+$ and Au^+ on the Au surface could be further tapped (Lin and Tseng 2010). Although copper (Cu) is an integral part of a number of enzymes and involved in many vital biochemical processes, chronic Cu overload or exposure to excess Cu leads to abnormal Cu metabolism and fatal neurodegenerative changes (Gaetke and Chow 2003). Glutathione-protected AuNCs were used for the efficient detection of cupric ions (Cu^{2+}) based on aggregation-induced fluorescent quenching and it was recovered through the addition of a strong metal ion chelator, ethylene diamine tetra acetate (EDTA) (Chen et al. 2009). AuNCs stabilized by an iron binding transferrin family protein, lactoferrin (Lf) was also used for the effective and sensitive detection of Cu^{2+} (Xavier et al. 2010). Near-infrared luminescent AuNPs (NIRL-AuNPs) were synthesized by heat-assisted reduction of a gold (I)-thiol complex as a sensor for Cu^{2+} quantification (Tu et al. 2011).

Simultaneous detection of both Hg^{2+} and Cu^{2+} ions through fluorescence quenching was achieved through BSA-conjugated AuNCs. EDTA and sodium borohydride (NaBH_2) were used as masking reagents, in which EDTA complexed with Cu^{2+} , and borohydride reduced Hg^{2+} which eliminated quenching effect, thus detection of the other ion was achieved (Cao et al. 2013). Glutathione-capped Au/Ag nanoclusters (GS-Au/AgNCs) by microwave irradiation had an efficient sensing property to detect many analytes such as Cu^{2+} , sulfide, iodide, cysteine, and glutathione (Zhang et al. 2015). In a promising study, Annie et al. (2012) employed l-3,4-dihydroxyphenylalanine (L-DOPA) capped AuNCs for the sensitive detection of Fe^{3+} with a limit of detection of $3.5 \mu\text{M}$ which is much lower than the maximum level (0.3 mgL^{-1} equivalent to $5.4 \mu\text{M}$) of Fe^{3+} permitted in drinking water by the U.S. Environmental Protection Agency. Screening of food materials for possible heavy metal contamination requires special consideration as a potent health issue, hence AuNC based sensing probes needs to be further explored to effectively handle the issues.

4.2.2 Biosensors

Carefully engineered AuNCs were observed to be capable for the efficient detection of various bio-macromolecules and other small molecules such as enzymes (Hu et al. 2012; Wen et al. 2013), folic acid (Hemmtenejad et al. 2014), proteins (Lin et al. 2013b; Selvaprakash and Chen 2014), dopamine (Tao et al. 2013; Aswathy and Sony 2014), cholesterol (Chen and Baker 2013) etc. The pioneering work in which AuNCs were used for detecting cellular proteins reported by Triulzi et al. (2006) used polyclonal, goat-derived anti-human IgG antibody conjugated PAMAM-AuNCs for the human IgG immunoassay. Huang et al. (2008) reported a new method using Platelet-derived growth factor AA (PDGF AA) modified fluorescent AuNCs (PDGF AA-L (AuND)) and PDGF binding aptamer modified AuNPs (Apt-Q (AuNP)) for the effective breast cancer specific protein detection. Fluorescence of PDGF AA-L(AuND) was quenched due to Apt-Q(AuNP) binding and addition of PDGFs, caused a decrease in interaction between Apt-Q(AuNP) and PDGF AA-L(AuND) which results in recovered fluorescence. Fluorescent mannose coated AuNCs were effectively used for the detection of Concanavalin A (Con A) and *Escherichia coli* (*E. coli*) wherein the fluorescence was increased after binding to corresponding proteins such as (Con A) and FimH of type 1 in *E. coli* (Huang et al. 2009). Serum glucose could be easily quantitated using cysteine stabilized AuNCs and the method is devoid of interference with other serum proteins (Hussain et al. 2011) and hence could be advantageous over the current colorimetric methods. Constant monitoring of rifampicin or rifampin (R), a common drug generally prescribed for long-term administration under regulated doses to treat inactive meningitis, cholestatic pruritus and tuberculosis (TB), is necessary to control the side effects and prevent overdose caused by chronic medication. Chatterjee et al. (2015) developed an efficient colorimetric assay for the detection of rifampicin in urine in which fluorescence of immobilized BSA-AuNCs on wax-printed papers was quenched by the increasing concentration of rifampicin.

5 Future Scopes of Fluorescent AuNCs

Many simple strategies have been formulated for the preparation of AuNCs from Au³⁺ in the presence of small biological molecules which acts as reducing and stabilizing agents. Despite the fact that the nature and concentration of the ligand, reaction temperature, time, solution pH, ionic strength and other parameters play significant roles in determining the formation of AuNCs with desirable physical, chemical and optical properties, they can be tuned for the fabrication of NCs for more sensitive fluorescence energy transfer based techniques. AuNCs have a few favourable circumstances as nanoprobe attributable to their great stability and mono-dispersion in the physiological environment which will lead to enhanced

sensitivity and increased tracking lifetime. Since AuNCs have the remarkable biocompatibility, it could be suited for *in vitro* and *in vivo* applications. AuNC-based platforms can be utilized to improve or empower a wide assortment of treatments including drug delivery, nucleic acid delivery, photothermal ablation, radiotherapy and real time fluorescent imaging. The capacity to tune the size, shape and thus the physical properties of NCs, alongside their low cytotoxicity, high biocompatibility, and scope of surface modulations, makes them promising contender for clinical use. It is sensible to trust that increasingly delicate and specific detection and imaging procedures utilizing Au based NCs will soon get to be brilliant measures for clinical applications.

In-depth molecular imaging and complete surgical resection of malignant tissue is still a challenging task in oncology (Kelderhouse et al. 2013; Nguyen and Tsien 2013). Even though semiconductor quantum dots (QDs) offered great assurance in early cancer detection and diagnosis due to its intense, stable fluorescence (Smith et al. 2006; Alivisatos et al. 2005; Michalet et al. 2005), its wide spread usage is heavily limited owing to the higher risk to human health as well as environment due to its heavy metal content (Hardmen 2006; Tsoi et al. 2013). Organic dyes used for imaging purpose are greatly liable to photo bleaching which makes them unsuitable for long term usage (Li et al. 2014; Jaiswal et al. 2003; Chen and Gerion 2004). AuNCs as an emerging fluorescent nanomaterial can overcome most of these disadvantages of quantum dots and organic dyes (Lin et al. 2009b; Qu et al. 2015) and have a greater potential for many applications in biomedical field (Lin et al. 2010). AuNCs synthesized by green-chemistry possessed greater water-solubility, high photostability, large Stokes shift, ultrasmall size, nontoxicity, and good biocompatibility and hence could be carefully tuned for diverse applications in biomedical field (Wang et al. 2011b; Qu et al. 2015; Muhammed et al. 2010). The surface modification of AuNCs using tumor specific ligands will offer targeted imaging and drug delivery (Huang et al. 2009; Huang et al. 2011a) thereby extending its promising role in personalized medicine. Functional molecules present as the capping agents in AuNCs will support conjugation of targeting molecules and chemotherapeutics for its efficient delivery at the tumor site (Shang et al. 2011b). Folic acid conjugated AuNCs (NCs-FA) highlighted the potential of AuNCs to become a diagnostic tool for cancer detection and imaging (Hu et al. 2014). Fluorescent AuNCs conjugated with diatrizoic acid and AS1411 aptamer (AS1411-DA-AuNPs) with nucleolin specific targeting function make NCs as a powerful tool in the field of fluorescence-guided surgery (Li et al. 2015a). Doxorubicin immobilized multifunctional AuNCs (Au-Met-DOX) and Herceptin conjugated AuNCs (AuNCs-Her) confirmed the promising future of AuNCs as a drug carrier with at most specificity and target ability (Chen et al. 2012; Wang et al. 2011b). Although marvelous transitions are undergoing in the study of AuNCs as promising multifunctional optical probes for molecular imaging and therapy, most studies are mainly concentrating on *in vitro* (Shang et al. 2011b; Muhammed et al. 2009; Qiao et al. 2013; Vankayala et al. 2015; Chen et al. 2012) applications than *in vivo* (Wu et al. 2010) real time uses. Further detailed *in vivo* and preclinical to clinical investigations are warranted to establish the full potential of AuNCs for myriad applications aiming in the betterment of human life.

6 Versatile Biomedical Applications of Other Gold Nanomaterials

Gold nanoparticles can be manufactured into a variety of forms, comprising of gold nanospheres, nanorods (AuNRs), nanoshells, nanobelts, nanocages, nanoprisms, nanotubes (Nandini et al. 2014, 2016a) nanoribbons (Nandini et al. 2016b) and nanostars (Fig. 8). Many processes have been developed to synthesize gold nanomaterials, including both chemical methods (e.g., chemical reduction, photochemical reduction, co-precipitation, thermal decomposition, hydrolysis, etc.) and physical methods (e.g., vapor deposition, laser ablation, grinding and many more).

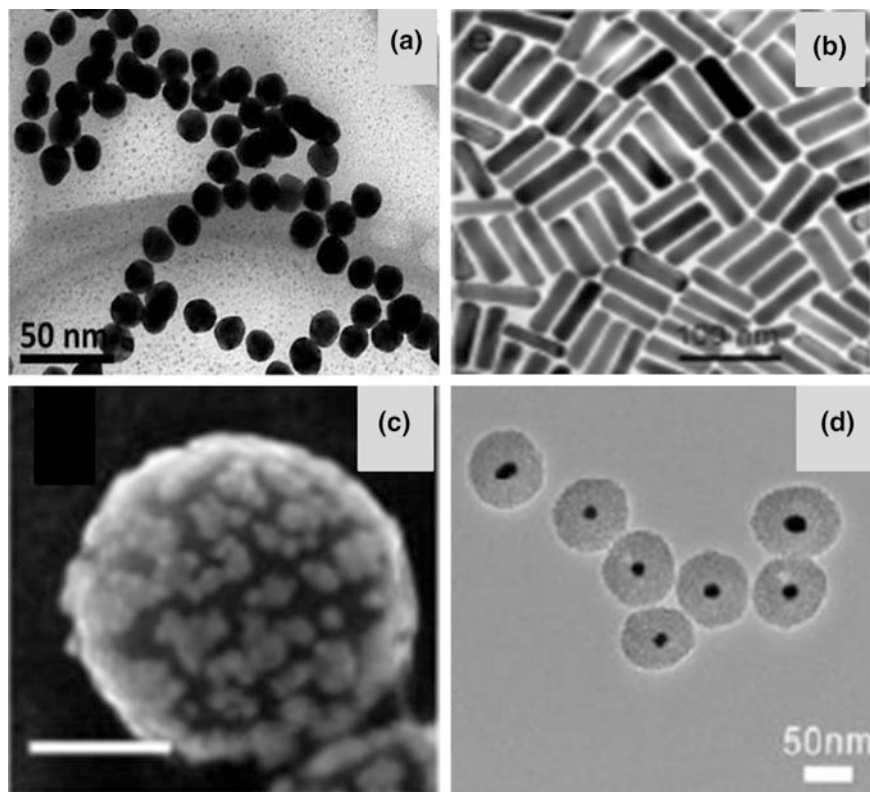


Fig. 8 **a** Electron microscopy of Au-citrate nanoparticles (Reprinted with permission from Plascencia-Villa et al. (2015) © 2015 American Chemical Society). **b** TEM images of silica-coated AuNRs. Scale bars correspond to 100 nm (Reprinted with permission from Jia et al. (2015) © 2015 American Chemical Society). **c** SEM image gold nanoshells on silica core particles. Scale bars correspond to 100 nm (Reprinted with permission from Sauerbeck et al. (2014) © 2014 American Chemical Society). **d** TEM image of gold nanospheres coated with mesoporous silica (Au@mSiO₂-TTA) (Reprinted with permission from Song et al. (2015) © 2015 American Chemical Society)

The ultimate goal of every process is to obtain nanomaterials with a high level of homogeneity and provide fine control over size, shape and surface properties (Feldheim and Foss 2011). Such nanomaterials have attracted diverse role in biomedical field such as targeted imaging, drug delivery, photo dynamic and photo thermal therapy etc. These gold nanomaterials exhibit localized SPR effect because of it is much smaller in size than the light wavelength and its chemical, physical and optical properties depend on its size and shape which is different from bulk gold (Mie 1908). Gold nanomaterials of approximately 3–20 nm display light absorption but at 20–80 nm exhibit an increasing scattering/absorption ratio which gives great opportunity for biomedical imaging based on light scattering.

6.1 Contrast Agents

The plasmon absorption band varies on its shape and number from spherical to non-spherical NPs. Spherical AuNPs possesses only one plasmon absorption band. Different plasmon absorption bands of single NPs provides more information than a single visible band of spherical AuNPs (Liz Marzan 2006; Boisselier and Astruc 2009). AuNRs possess two plasmon bands, one in transverse and the other in longitudinal direction and its ratio is adjusted to shift the plasmon band to the NIR region which allows penetration into living tissues and avoid background fluorescence noise. Gold nanoshells are concentric spherical constructs consist of a thin outer gold shell and a silica core and its optical properties can be tuned by changing the core-shell ratio as well as the overall size and shape. Hence the absorption and scattering properties of AuNRs, gold nanospheres and gold nanoshell could be tuned to NIR region where blood and tissues are maximally transmissive. The specific tunable optical properties of these gold nanomaterials make it as ideal candidates for in vitro and in vivo imaging and photothermal therapy (Loo et al. 2005; Lin et al. 2006; Lal et al. 2008). It could also be used as contrast agents for optical coherence tomography (OCT) (Chen et al. 2005), photoacoustic tomography (PA) (Li et al. 2008; Yang et al. 2009; Kim et al. 2010), computed tomography (CT) (Hainfeld et al. 2006; Popovtzer et al. 2008; Maltzahn 2009), multi-photon microscopy, Surface-enhanced Raman spectroscopy (SERS), (Qian et al. 2008; Zavaleta et al. 2009) and Magnetic resonance imaging (MRI) (Lim et al. 2007; Eun et al. 2010). Optical imaging of epithelial growth factor receptor (EGFR) over expressed cervical epithelial cancer cells (SiHa cells) using monoclonal antibody conjugated AuNPs was achieved by Sokolov et al. (2003). In a similar work, immune-targeted AuNPs against EGFR was effectively utilized for imaging purpose in non-malignant epithelial cell line (HaCaT) and two malignant oral epithelial cell lines (HOC 313 clone 8 and HSC 3). Cancerous cells displayed a higher uptake of the NP which was colored in SPR scattering image with dark background using a white-light source from a conventional microscope (El-Sayed et al. 2005).

Gold is a new-age selective X-ray contrast agent which could be effectively exploited in early cancer diagnostics due to its greater X-ray attenuation ability

compared with iodine, which is currently used as a contrast agent (Hainfeld et al. 2006). Although X-ray based computed tomography (CT) is one of the most convenient imaging/diagnostic tools, it is not considered as molecular imaging tool since targeted and molecularly specific contrast agents for CT is not suitably established. Popovtzer et al. (2008) demonstrated a new CT imaging modality in head and neck cancer which enables, cancer detection at the cellular and molecular level with standard clinical CT using gold nano-probes that selectively target tumor specific antigen and inducing distinct contrast in CT imaging. Hybrid nanoparticles with superparamagnetic iron oxide embedded in AuNP shells displayed combined applications in MRI and optical imaging, photothermal therapy and targeted cancer therapy. Iron core of this NPs provides strong T2 (spin-spin relaxation time) contrast, while Au part act as optical contrast agent (Lim et al. 2007; Larson et al. 2007; Ji et al. 2007). The hybrid NPs targeted to the epidermal growth factor receptor (EGFR), demonstrated fascinating effects in MDA-MB-468 breast cancer cells (Larson et al. 2007).

Rayleigh scattering of AuNRs are excellent and hence could enhance SERS due to surface plasmon field overlap. Anti-epidermal growth factor receptor (anti-EGFR) antibodies conjugated AuNRs specifically bind to human oral cancer cells and gave enhanced Raman spectrum useful for diagnostic purpose (Huang et al. 2007b). Similarly, Lee et al. (2007) demonstrated the potential feasibility of SERS imaging in live human embryonic kidney cells HEK293 expressing PLCgamma1 using monoclonal antibody conjugated Au/Ag core-shell nanoparticles. Bi-functional poly ethylene glycol (PEG) coated AuNPs were covalently coupled to F19 monoclonal antibodies for the staining of resected human pancreatic adenocarcinoma cells and visualized by darkfield microscopy near the nanoparticle resonance scattering maximum (Eck et al. 2008). AuNRs functionalized with Herceptin (Her-PEG-GNRs) was used for in vivo targeting of breast cancer specific antigens. It demonstrated significant stability and targetability in vitro in the presence of blood and then in vivo in nude mice model for breast cancer. These observations could effectively translate AuNRs as a powerful molecular imaging agent (Eghedari et al. 2009). Two-photon luminescence (TPL) intensity of AuNRs at 830 nm excitation on a far-field laser-scanning microscope was 58 times than that from a single rhodamine molecule and hence could be adopted for applications as TPL imaging agents. A simple colorimetric method was developed for the visual distinction between cancerous cells and normal ones using aptamer-conjugated AuNPs, in which cancer cells displayed a distinct color change compared with the normal cells (Medley et al. 2008).

6.2 Photothermal Therapy

Although chemotherapy holds the major share in cancer treatment regimen it is often accompanied with dramatic side effects; surgical removal of tumors limited to accessible solid tumors only and radiotherapy also affect healthy surrounding tissue

along the radiation path. Photothermal therapy is an emerging technique that uses optical sources to generate heat to destroy tumor cells. Among the gold nanomaterials; AuNRs, gold nanospheres and gold nanoshells absorb light in a broad spectrum range from near UV to NIR, but the NIR region is especially crucial in order to penetrate inside living tissues (Jain et al. 2007). Chemotherapeutic molecules conjugated photothermal agents can decipher better outcome because laser hypothermia induced drug release is possible at the tumor site (photo-chemotherapy).

PEG coated gold nanoshells with peak optical absorption in the NIR was effectively employed for the photothermal therapy in murine colon carcinoma (CT26WT) tumor bearing immune-competent mice, wherein tumors were illuminated with a diode laser for hyperthermia generation (O'Neal et al. 2004). Focused pulsed NIR laser irradiation of phosphatidylcholine-passivated gold nanorods (PC-NRs) achieved selective killing of single cells (Takahashi et al. 2006). Folate conjugated AuNRs renders the extensive blebbing of KB cells when irradiated with femto second Ti:sapphire laser (Huff et al. 2007). Anti-epidermal growth factor receptor (anti-EGFR) conjugated AuNPs and gold nanoshells were used for tumor targeted hyperthermia (El-Sayed et al. 2006; Huang et al. 2006). Similarly, prostate cancer ablation (PC-3 cell) in nude mice model were reported using 110 nm gold nanoshell, irradiated with 810 nm NIR laser at the spot site (Stern et al. 2008). NF-kappaB is a transcription factor critically involved in tumor formation and progression. Folate receptor conjugated gold nanospheres carrying siRNA recognizing NF-kappaB p65 subunit were synthesized for the successful down-regulation of NF-kappaB in cancer cells after NIR light irradiation (Lu et al. 2010). A dual-functional nanoparticle that mediates simultaneous photothermal cell killing and controllable drug release for complete reduction of tumor was devised, in which doxorubicin was loaded into hollow gold nanospheres (HAuNS) coated with PEG. The nano construct advertised superior anti-tumor activity than free DOX, NP3, or liposomal DOX in the in vitro and in vivo using human breast cancer MDA-MB-231 and ovarian cancer A2780 cells (You et al. 2010, 2012).

6.3 Drug Carriers

The increased surface to volume ratio of the nanoparticles allows the conjugation of targeting moieties with high drug loading which will ultimately enhance the therapeutic efficacy. Synthesis of gold nanomaterials using biological materials such as proteins, polysaccharides, microorganisms, plant extracts, cell extracts and many more predominate in biomedical applications because of its biocompatibility and non-toxicity (Joseph and Sreelekha 2014). NP based drug-delivery systems for cancer therapeutics are swiftly evolving to overcome the drug resistances of Cancer Stem Cells (CSC). Recently, NP-based strategies have illustrated promising therapeutic efficacy while reducing adverse effects, compared with those of conventional therapy (Joseph et al. 2016). Destruction of tumor mass by NPs targeting

both CSCs and cancer cells with possibly eliminate the tumor burden and also block any tumor relapse.

Gold nanomaterials have been well explored as a promising drug delivery vehicle for cancer in recent years. Multidrug resistance (MDR) is a major obstacle during chemotherapy of cancer in which drug efflux affects the therapy. AuNPs-doxorubicin (Au-PEG-SS-DOX) conjugates were developed to overcome MDR in cancer cells (Gu et al. 2011). Similarly, doxorubicin conjugated onto the surface of AuNPs with a PEG spacer via an SMCC linker also demonstrated highly efficient cellular entry and enhanced cytotoxicity in multidrug resistant HepG2-R cancer cells compared with free doxorubicin (Cheng et al. 2013). In another promising work, rifampicin (RF) which was known to reduce the MDR was conjugated to AuNPs to enhance the rate as well as efficiency of endocytosis of NPs in cancer cells which could lead to demand of decreased amount of AuNPs for cancer management (Ali et al. 2014). Anticancer and immuno-modulatory polysaccharide PST001 isolated from the seed kernels of *Tamarindus indica* acted both as reducing and capping agent for the preparation of PST-Gold nanoparticles (Joseph et al. 2013). The resultant nanoparticles showed high stability with no obvious aggregation for months and a broader range of pH tolerance. The nanoconjugate was effective against various human cancer cell lines and exhibited induction of apoptosis. Importantly, PST-Gold nanoparticles demonstrated significant increase in the life span of tumor-challenged mice models and displayed greater reduction in the tumor volume in both ascites and solid tumours (Joseph et al. 2014).

Methotrexate (MTX) conjugated AuNPs (MTX-AuNP) was found to be more effective than free drug in overcoming MDR (Chen et al. 2007). Similarly, Brown et al. (2010) synthesized oxaliplatin conjugated AuNPs which exhibited increased cytotoxicity, drug uptake, and localization in the A549 lung epithelial cancer cell lines and the colon cancer cell lines HCT116, HCT15, HT29 and RKO than free drug. In a more engineered fashion, DOX, tumor targeting ligand (cyclo (Arg-Gly-Asp-D-Phe-Cys) peptides, (cRGD)) and ^{64}Cu -chelators were conjugated to the PEGylated AuNRs via hydrazone bond for targeted anticancer drug delivery and positron emission tomography (PET) imaging of tumors. These multifunctional NPs triggers pH-sensitive controlled drug release and in vivo PET imaging (Xiao et al. 2012). In a similar way multifunctional theranostic nanoparticle was developed using amphiphilic AuNPs coated with a Raman reporter BGLA (2-(4-(bis(4-(diethylamino)phenyl)(hydroxymethyl)phenoxy)ethyl 5-(1,2-dithio-lan-3-yl)pentanoate) for cancer targeted drug delivery. DOX was loaded on the as prepared nanoparticles and tagged with HER2 antibody as targeting drug moiety for specific tumor recognition. These nanoparticles trigger pH-sensitive drug release and SERS imaging (Song et al. 2012).

AuNPs was used as a vector for the targeted delivery of tumor necrosis factor (TNF) in MC-38 colon carcinoma tumors in mice and displayed superior tumor localization. It was found to be less toxic and more effective in reducing tumor burden than native TNF since maximal antitumor responses were achieved at lower doses of drug (Paciotti et al. 2004). PEGylated colloidal gold-TNF construct (CYT-6091) was tested in a phase I dose escalation clinical trial in advanced stage

cancer patients and found to be non-toxic compared to the doses of free recombinant human tumor necrosis factor alpha (rhTNF) (Libutti et al. 2010). In a similar study, PEG coated AuNPs incorporated with TNF-alpha payload and combined heating were studied in SCK mammary carcinomas grown A/J mice and found to decrease tumor growth (Visaria et al. 2006).

7 Conclusion

Gold based nanomaterials are one of the most widely studied molecules in the last decade, and are emerging as promising agents in cancer management in which fluorescent AuNCs holds a prominent position. Fluorescent AuNCs can be fabricated using many biological and organic materials as reducing and capping agents and the properties depends to the fabrication strategies adopted. AuNCs can overcome biological barriers and transport drugs to the tumor site and are potential alternatives to QDs and fluorophores which can enable early imaging, diagnosis and targeted therapy of cancer. Advances in genomics and proteomics provided accurate information about the expression of various receptors on cancers and hence different targeting moieties as well as chemotherapeutic agents could be conjugated to the surface of AuNCs for rapid and accurate tumor diagnosis and therapy. AuNCs could be used for combinatorial imaging with MRI, PET and CT for more potential tumor imaging. Although many reports suggest the biocompatible and non-toxic nature of AuNCs, detailed toxicity studies in suitable animal models are in infancy stage to make a stable conclusion about the safety in the wide spread use of this materials. Other forms of gold nanomaterials such as gold nanospheres, nanorods, nanoshells, nanobelts, nanocages, nanoprisms and nanostars also play much promising role in every aspect of human inference. In the pursuit of current knowledge, in the future of nanomedicine, AuNCs will be one of the innovative platforms for cancer diagnosis and treatment for improved patient survival outcome. Progresses in the fabrication of different useful nanomaterials and AuNCs might advantage for the advancement of more delicate fluorescence based strategies. It is our solid conviction that more sensitive and specific detecting and imaging systems utilizing Au based NCs will soon get to be brilliant principles for clinical applications.

References

- Ali MRK, Panikkanvalappil SR, El-Sayed MA (2014) Enhancing the efficiency of gold nanoparticles treatment of cancer by increasing their rate of endocytosis and cell accumulation using rifampicin. *J Am Chem Soc* 136(12):4464–4467. doi:10.1021/ja4124412
- Alivisatos A, Gu W, Larabell C (2005) Quantum dots as cellular probes. *Annu Rev Biomed Eng* 7:55–76

- Alvarez MM, Khoury JT, Schaaff TG et al (1997) Optical absorption spectra of nanocrystal gold molecules. *J Phys Chem B* 101(19):3706–3712
- Annie Ho JA, Chang HC, Su WT (2012) DOPA-mediated reduction allows the facile synthesis of fluorescent gold nanoclusters for use as sensing probes for ferric ions. *Anal Chem* 84(7):3246–3253
- Apell P, Monreal R, Lundqvist S (1988) Photoluminescence of noble metals. *Phys Scr* 38(2):174–179
- Aswathy B, Sony G (2014) Cu²⁺ modulated BSA-Au nanoclusters: a versatile fluorescence turn-on sensor for dopamine. *Microchem J* 116:151–156. doi:[10.1016/j.microc.2014.04.016](https://doi.org/10.1016/j.microc.2014.04.016)
- Bao Y, Zhong C, Vu DM et al (2007) Nanoparticle-free synthesis of fluorescent gold nanoclusters at physiological temperature. *J Phys Chem C* 111(33):12194–12198
- Barnes WL, Dereux A, Ebbesen TW (2003) Surface plasmon subwavelength optics. *Nature* 424(6950):824–830
- Bhattacharya D, Gupta RK (2005) Nanotechnology and potential of microorganisms. *Crit Rev Biotechnol* 25(4):199–204
- Bigioni TP, Whetten RL, Dag O (2000) Near-infrared luminescence from small gold nanocrystals. *J Phys Chem B* 104(30):6983–6986
- Boisselier E, Astruc D (2009) Gold nanoparticles in nanomedicine: preparations, imaging, diagnostics, therapies and toxicity. *Chem Soc Rev* 38:1759–1782. doi:[10.1039/B806051G](https://doi.org/10.1039/B806051G)
- Brown S, Sarikaya M, Johnson E (2000) A genetic analysis of crystal growth. *J Mol Biol* 299(3):725–735
- Brown SD, Nativo P, Smith JA et al (2010) Gold nanoparticles for the improved anticancer drug delivery of the active component of oxaliplatin. *J Am Chem Soc* 132(13):4678–4684
- Cao D, Fan J, Qiu J et al (2013) Masking method for improving selectivity of gold nanoclusters in fluorescence determination of mercury and copper ions. *Biosens Bioelectron* 42C(1):47–50. doi:[10.1016/j.bios.2012.10.084](https://doi.org/10.1016/j.bios.2012.10.084)
- Chatterjee K, Kuo CW, Chen A et al (2015) Detection of residual rifampicin in urine via fluorescence quenching of gold nanoclusters on paper. *J Nanobiotechnol* 13:46. doi:[10.1186/s12951-015-0105-5](https://doi.org/10.1186/s12951-015-0105-5)
- Chen X, Baker GA (2013) Cholesterol determination using protein-templated fluorescent gold nanocluster probes. *Analyst* 138(24):7299–7302
- Chen FQ, Gerion D (2004) Fluorescent CdSe/ZnS nanocrystal-peptide conjugates for long-term, nontoxic imaging and nuclear targeting in living cells. *Nano Lett* 4:1827–1832
- Chen CL, Rosi NL (2010) Peptide-based methods for the preparation of nanostructured inorganic materials. *Angew Chem Int Ed* 49(11):1924–1942
- Chen TH, Tseng WL (2012) (Lysozyme type VI)-stabilized Au 8 clusters: synthesis mechanism and application for sensing of glutathione in a single drop of blood. *Small* 8(12):1912–1919
- Chen SW, Ingram RS, Hostetler MJ et al (1998) Gold-nano electrodes of varied size: transition to molecule-like charging. *Science* 28(5372):2098–2101
- Chen J, Saeki F, Wiley BJ et al (2005) Gold nanocages: bioconjugation and their potential use as optical contrast agents. *Nano Lett* 5(3):473–477. doi:[10.1021/nl047950t](https://doi.org/10.1021/nl047950t)
- Chen Y, Tsai C, Huang P et al (2007) Methotrexate conjugated to gold nanoparticles inhibits tumor growth in a syngeneic lung tumor model. *Mol Pharm* 4(5):713–722
- Chen WB, Tu XJ, Guo XQ (2009) Fluorescent gold nanoparticles-based fluorescence sensor for Cu²⁺ ions. *Chem Commun* 13:1736–1738. doi:[10.1039/B820145E](https://doi.org/10.1039/B820145E)
- Chen H, Li B, Ren X et al (2012) Multifunctional near-infrared-emitting nano-conjugates based on gold clusters for tumor imaging and therapy. *Biomaterials* 33:8461–8476
- Chen Y, Wang Y, Wang C et al (2013) Papain-directed synthesis of luminescent gold nanoclusters and the sensitive detection of Cu²⁺. *J Colloid Interface Sci* 396:63–68. doi:[10.1016/j.jcis.2013.01.031](https://doi.org/10.1016/j.jcis.2013.01.031)
- Chen LY, Wang CW, Yuan Z et al (2014) Fluorescent gold nanoclusters: recent advances in sensing and imaging. *Anal Chem* 87(1):216–229
- Cheng J, Gu YJ, Cheng SH et al (2013) Surface functionalized gold nanoparticles for drug delivery. *J Biomed Nanotechnol* 9(8):1362–1369

- Chevrier DM, Chatt A, Zhang P (2012) Properties and applications of protein-stabilized fluorescent gold nanoclusters: short review. *J Nanophoton* 6:064504. doi:[10.1117/1.JNP.6.064504](https://doi.org/10.1117/1.JNP.6.064504)
- Choi YE, Kwak JW, Park JW (2010) Nanotechnology for early cancer detection. *Sensors* 10(1):428–455
- Couvreur P, Vauthier C (2006) Nanotechnology: intelligent design to treat complex disease. *Pharm Res* 23(7):1417–1450
- Crookes-Goodson WJ, Slocik JM, Naik RR (2008) Bio-directed synthesis and assembly of nanomaterials. *Chem Soc Rev* 37(11):2403–2412
- Ding H, Liang C, Sun K et al (2014) Dithiothreitol-capped fluorescent gold nanoclusters: An efficient probe for detection of copper (II) ions in aqueous solution. *Biosens Bioelectron* 59:216–220. doi:[10.1016/j.bios.2014.03.045](https://doi.org/10.1016/j.bios.2014.03.045)
- Duan HW, Nie NM (2007) Etching colloidal gold nanocrystals with hyperbranched and multivalent polymers: a new route to fluorescent and water-soluble atomic clusters. *J Am Chem Soc* 129(9):2412–2413. doi:[10.1021/ja067727t](https://doi.org/10.1021/ja067727t)
- Eck W, Craig G, Sigdel A et al (2008) PEGylated gold nanoparticles conjugated to monoclonal F19 antibodies as targeted labeling agents for human pancreatic carcinoma tissue. *ACS Nano* 2(11):2263–2272
- Eghtedari M, Liopo AV, Copland JA et al (2009) Engineering of hetero-functional gold nanorods for the in vivo molecular targeting of breast cancer cells. *Nano Lett* 9(1):287–291
- El-Sayed IH, Huang XH, El-Sayed MA (2005) Surface plasmon resonance scattering and absorption of anti-EGFR antibody conjugated gold nanoparticles in cancer diagnostics: applications in oral cancer. *Nano Lett* 5:829–834
- El-Sayed IH, Huang XH, El-Sayed MA et al (2006) Selective laser photo-thermal therapy of epithelial carcinoma using anti-EGFR antibody conjugated gold nanoparticles. *Cancer Lett* 239:129–135
- Eun CC, Charles G, Jingyi C et al (2010) Inorganic nanoparticle-based contrast agents for molecular imaging. *Trends Mol Med* 16(12):561–573
- Feldheim DL, Foss CA (2001) Metal nanoparticles synthesis, characterization, and applications. Marcel Dekker, New York
- Fendler JH (1997) Biomineralization inspired preparation of nanoparticles and nanoparticulate films. *Curr Opin Solid St M* 2(3):365–369
- Ferrari M (2005) Cancer nanotechnology: opportunities and challenges. *Nat Rev Cancer* 5(3):161–171
- Frank M, Schloissnig S (2010) Bioinformatics and molecular modeling in glycobiology. *Cell Mol Life Sci* 67(16):2749–2772. doi:[10.1007/s00018-010-0352-4](https://doi.org/10.1007/s00018-010-0352-4)
- Gaetke LM, Chow CK (2003) Copper toxicity, oxidative stress, and antioxidant nutrients. *Toxicology* 189(1–2):147–163
- Galib Mayur B, Prajapati PK (2011) Therapeutic potentials of metals in ancient India: a review through Charaka Samhita. *J Ayurveda Integr Med* 2(2):55–63
- Gao S, Chen D, Li Q et al (2014) Near-infrared fluorescence imaging of cancer cells and tumors through specific biosynthesis of silver nanoclusters. *Sci Rep* 4:4384. doi:[10.1038/srep04384](https://doi.org/10.1038/srep04384)
- Garcia AR, Rahn I, Johnson S et al (2013) Human insulin fibril-assisted synthesis of fluorescent gold nanoclusters in alkaline media under physiological temperature. *Colloids Surf B* 105:167–172. doi:[10.1016/j.colsurfb.2012.12.052](https://doi.org/10.1016/j.colsurfb.2012.12.052)
- Ge W, Zhang Y, Ye J et al (2015) Facile synthesis of fluorescent Au/Ce nanoclusters for high-sensitive bioimaging. *J Nanobiotechnol* 13:8. doi:[10.1186/s12951-015-0071-y](https://doi.org/10.1186/s12951-015-0071-y)
- Ghosh A, Udayabhaskarao T, Pradeep T (2012) One-step route to luminescent Au18SG14 in the condensed phase and its closed shell molecular ions in the gas phase. *J Phys Chem Lett* 3(15):1997–2002. doi:[10.1021/jz3007436](https://doi.org/10.1021/jz3007436)
- Grzelczak M, Perez-Juste J, Mulvaney P et al (2008) Shape control in gold nanoparticle synthesis. *Chem Soc Rev* 37:1783–1791. doi:[10.1039/B711490G](https://doi.org/10.1039/B711490G)
- Gu YJ, Cheng J, Man CWY et al (2011) Gold doxorubicin nanoconjugates for overcoming multidrug resistance. *Nanomedicine* 8(2):204–211

- Guevel XL, Daum N, Schneider M (2011) Synthesis and characterization of human transferrin-stabilized gold nanoclusters. *Nanotechnology* 22(27):275103. doi:[10.1088/0957-4484/22/27/275103](https://doi.org/10.1088/0957-4484/22/27/275103)
- Haberland H (1994) Clusters of atoms and molecules: theory experiment, and clusters of atoms. Springer-Verlag, Berlin
- Hainfeld JF, Slatkin D, Focella TM et al (2006) Gold nanoparticles: a new X-ray contrast agent. *British J Radiol* 79(939):248–253. doi:[10.1259/bjr/13169882](https://doi.org/10.1259/bjr/13169882)
- Hardman R (2006) A toxicologic review of quantum dots: toxicity depends on physicochemical and environmental factors. *Environ Health Perspect* 114(2):165–172
- Hemmateenejad B, Shakerizadeh-Shirazi F, Samari F (2014) BSA-modified gold nanoclusters for sensing of folic acid. *Sensors Actuators B* 199:42–46. doi:[10.1016/j.snb.2014.03.075](https://doi.org/10.1016/j.snb.2014.03.075)
- Hicks JF, Templeton AC, Chen S et al (1999) The monolayer thickness dependence of quantized double-layer capacitances of monolayer-protected gold clusters. *Anal Chem* 71(17):3703–3711
- Hicks JF, Miles DT, Murray RW (2002) Quantized double layer charging of highly monodisperse metal nanoparticles. *J Am Chem Soc* 124(44):13322–13328
- Hostetler MJ, Wingate JE, Zhong CJ et al (1998) Alkanethiolate gold cluster molecules with core diameters from 1.5 to 5.2 nm: core and monolayer properties as a function of core size. *Langmuir* 14(1):17–30
- Hu L, Han S, Parveen S et al (2012) Highly sensitive fluorescent detection of trypsin based on BSA stabilized gold nanoclusters. *Biosens Bioelectron* 32(1):297–299. doi:[10.1016/j.bios.2011.12.007](https://doi.org/10.1016/j.bios.2011.12.007)
- Hu D, Sheng Z, Fang S et al (2014) Folate receptor-targeting gold nanoclusters as fluorescence enzyme mimetic nanoprobe for tumor molecular colocalization diagnosis. *Theranostics* 4(2):142–153
- Huang T, Murray RW (2001) Visible luminescence of water-soluble monolayer-protected gold clusters. *J Phys Chem B* 105(50):12498–12502. doi:[10.1021/jp0041151](https://doi.org/10.1021/jp0041151)
- Huang XH, Jain PK, El-Sayed IH et al (2006) Determination of the minimum temperature required for selective photothermal destruction of cancer cells with the use of immunotargeted gold nanoparticles. *Photochem Photobiol* 82(2):412–417
- Huang CC, Yang Z, Lee KH et al (2007a) Synthesis of highly fluorescent gold nanoparticles for sensing mercury(II). *Angew Chem Int Ed* 46(36):6824–6828. doi:[10.1002/anie.200700803](https://doi.org/10.1002/anie.200700803)
- Huang XH, El-Sayed IH, Qian W et al (2007b) Cancer cells assemble and align gold nanorods conjugated to antibodies to produce highly enhanced, sharp, and polarized surface Raman spectra: a potential cancer diagnostic marker. *Nano Lett* 7(6):1591–1597
- Huang CC, Chiang CK, Lin ZH et al (2008) Bioconjugated gold nanodots and nanoparticles for protein assays based on photoluminescence quenching. *Anal Chem* 80(5):1497–1504. doi:[10.1021/ac701998f](https://doi.org/10.1021/ac701998f)
- Huang CC, Chen CT, Shiang YC et al (2009) Synthesis of fluorescent carbohydrate-protected Au nanodots for detection of Concanavalin A and *Escherichia coli*. *Anal Chem* 81(3):875–882. doi:[10.1021/ac8010654](https://doi.org/10.1021/ac8010654)
- Huang P, Xu C, Lin J et al (2011a) Folic acid-conjugated graphene oxide loaded with photosensitizers for targeting photodynamic therapy. *Theranostics* 1:240–250. doi:[10.7150/thno.v01p0240](https://doi.org/10.7150/thno.v01p0240)
- Huang X, Li B, Li B et al (2011b) Facile preparation of highly blue fluorescent metal nanoclusters in organic media. *J Phys Chem C* 116(1):448–455. doi:[10.1021/jp209662n](https://doi.org/10.1021/jp209662n)
- Huff TB, Tong L, Zhao Y et al (2007) Hyperthermic effects of gold nanorods on tumor cells. *Nanomedicine* 2(1):125–132. doi:[10.2217/17435889.2.1.125](https://doi.org/10.2217/17435889.2.1.125)
- Hussain AM, Sarangi SN, Kesarwani JA et al (2011) Au-nanocluster emission based glucose sensing. *Biosens Bioelectron* 29(1):60–65. doi:[10.1016/j.bios.2011.07.066](https://doi.org/10.1016/j.bios.2011.07.066)
- Jain P, El-Sayed IH, El-Sayed MA (2007) Au nanoparticles target cancer. *Nanotoday* 2(1):18–29
- Jaiswal JK, Mattoussi H, Mauro JM et al (2003) Long-term multiple color imaging of live cells using quantum dot bioconjugates. *Nat Biotechnol* 21:47–51. doi:[10.1038/nbt767](https://doi.org/10.1038/nbt767)

- Jao YC, Chen MK, Lin SY (2010) Enhanced quantum yield of dendrimer-entrapped gold nanodots by a specific ion pair association and microwave irradiation for bioimaging. *Chem Comm* 46 (15):2626–2628
- Ji X, Shao R, Elliott AM et al (2007) Bifunctional gold nanoshells with a superparamagnetic iron oxide-silica core suitable for both MR imaging and photothermal therapy. *J Phys Chem C* 111:6245–6251
- Jia H, Fang C, Zhu XM et al (2015) Synthesis of absorption-dominant small gold nanorods and their plasmonic properties. *Langmuir* 31:7418–7426. doi:[10.1021/acs.langmuir.5b01444](https://doi.org/10.1021/acs.langmuir.5b01444)
- Joseph MM, Sreelekha TT (2014) Gold nanoparticles—synthesis and applications in cancer management. *Recent Patents Mater Sci* 7(1):8–25
- Joseph MM, Aravind SR, Sheeja V et al (2013) PST-Gold nanoparticle as an effective anticancer agent with immunomodulatory properties. *Colloids Surf B* 104:32–39. doi:[10.1016/j.colsurfb.2012.11.046](https://doi.org/10.1016/j.colsurfb.2012.11.046)
- Joseph MM, Aravind SR, Sheeja V et al (2014) Antitumor activity of galactoxylglucan-gold nanoparticles against murine ascites and solid carcinoma. *Colloids Surf, B* 116:219–227. doi:[10.1016/j.colsurfb.2013.12.058](https://doi.org/10.1016/j.colsurfb.2013.12.058)
- Joseph MM, George SK, Sreelekha TT (2016) Bridging 'Green' with nanoparticles: biosynthesis approaches for cancer management and targeting of cancer stem cells. *Curr Nanosci* 12(1): 47–62
- Katti KK, Kattumuri V, Bhaskaran S et al (2009) Facile and general method for synthesis of sugar coated gold nanoparticles. *Int J Green Nanotechnol Biomed* 1(1):B53–B59. doi:[10.1080/19430850902983848](https://doi.org/10.1080/19430850902983848)
- Kawasaki H, Yamamoto H, Fujimori H et al (2010) Stability of the DMF-protected Au nanoclusters: photochemical, dispersion, and thermal properties. *Langmuir* 26(8):5926–5933. doi:[10.1021/la9038842](https://doi.org/10.1021/la9038842)
- Kawasaki H, Hamaguchi K, Osaka I et al (2011a) PH-dependent synthesis of pepsin-mediated gold nanoclusters with blue green and red fluorescent emission. *Adv Funct Mater* 21(18):3508–3515. doi:[10.1002/adfm.201100886](https://doi.org/10.1002/adfm.201100886)
- Kawasaki H, Yoshimura K, Hamaguchi K et al (2011b) Trypsin-stabilized fluorescent gold nanocluster for sensitive and selective Hg₂⁺ detection. *Anal Sci* 27(6):591–596
- Kelderhouse LE, Chelvam V, Wayua C et al (2013) Development of tumor-targeted near infrared probes for fluorescence guided surgery. *Bioconjug Chem* 24(6):1075–1080. doi:[10.1021/bc400131a](https://doi.org/10.1021/bc400131a)
- Kennedy TAC, MacLean JL, Liu J et al (2012) Blue emitting gold nanoclusters templated by poly-cytosine DNA at low pH and poly-adenine DNA at neutral pH. *Chem Commun* 48 (54):6845–6847
- Kim C, Cho EC, Chen J et al (2010) In vivo molecular photoacoustic tomography of melanomas targeted by bioconjugated gold nanocages. *ACS Nano* 4(8):4559–4564. doi:[10.1021/nn100736c](https://doi.org/10.1021/nn100736c)
- Kong Y, Chen J, Gao F, Brydson R et al (2013) Near-infrared fluorescent ribonuclease-A-encapsulated gold nanoclusters: preparation, characterization, cancer targeting and imaging. *Nanoscale* 5(3):1009–1017. doi:[10.1039/c2nr32760k](https://doi.org/10.1039/c2nr32760k)
- Kreibig U, Vollmer M (1995) *Optical properties of metal clusters*. Springer, Berlin
- Kryachko ES, Remade F (2005a) Complexes of DNA bases and gold clusters Au₃ and Au₄ involving nonconventional N-H...Au hydrogen bonding. *Nano Lett* 5(4):735–739. doi:[10.1021/nl050194m](https://doi.org/10.1021/nl050194m)
- Kryachko ES, Remade F (2005b) Complexes of DNA bases and Watson-Crick base pairs with small neutral gold clusters. *J Phys Chem B* 109(48):22746–22757
- La Bean TH, Li HY et al (2007) Constructing novel materials with DNA. *Nano Today* 2(2):26–35. doi:[10.1016/S1748-0132\(07\)70056-7](https://doi.org/10.1016/S1748-0132(07)70056-7)
- Lal S, Clarell SE, Halas NJ et al (2008) Nanoshell-enabled photothermal cancer therapy: impending clinical impact. *Acc Chem Res* 41(12):1842–1851. doi:[10.1021/ar800150g](https://doi.org/10.1021/ar800150g)

- Larson TA, Bankson J, Aaron J et al (2007) Hybrid plasmonic magnetic nanoparticles as molecular specific agents for MRI/optical imaging and photothermal therapy of cancer cells. *Nanotechnology* 18(32):325101
- Le GX, Daum N, Schneider (2011) Synthesis and characterization of human transferrin-stabilized gold nanoclusters. *Nanotechnology* 22(27):275103. doi:[10.1088/0957-4484/22/27/275103](https://doi.org/10.1088/0957-4484/22/27/275103)
- Lee D, Donkers RL, Wang G et al (2004) Electrochemistry and optical absorbance and luminescence of molecule-like Au₃₈ nanoparticles. *J Am Chem Soc* 126(19):6193–6199
- Lee S, Kim S, Choo J et al (2007) Biological imaging of HEK293 cells expressing PLCγ1 using surface-enhanced Raman microscopy. *Anal Chem* 79(3):916–922
- Li PC, Wang CRC, Shieh DB et al (2008) In vivo photoacoustic molecular imaging with simultaneous multiple selective targeting using antibody-conjugated gold nanorods. *Opt Express* 16(23):18605–18615. doi:[10.1364/OE.16.018605](https://doi.org/10.1364/OE.16.018605)
- Li J, Zhu J, Xu K (2014) Fluorescent metal nanoclusters: from synthesis to applications. *Trends Anal Chem* 58:90–98. doi:[10.1016/j.trac.2014.02.011](https://doi.org/10.1016/j.trac.2014.02.011)
- Li CH, Kuo TR, Su HJ et al (2015a) Nanoparticles with computed tomography imaging accesses for in vivo tumor resection. *Sci Rep* 5:15675. doi:[10.1038/srep15675](https://doi.org/10.1038/srep15675)
- Li ZY, Wu YT, Tseng WL (2015b) UV-light-induced improvement of fluorescence quantum yield of DNA-templated gold nanoclusters: application to ratiometric fluorescent sensing of nucleic acids. *ACS Appl Mater Interfaces* 7(42):23708–23716. doi:[10.1021/acsami.5b07766](https://doi.org/10.1021/acsami.5b07766)
- Libutti SK, Paciotti GF, Byrnes AA et al (2010) Phase I and pharmacokinetic studies of CYT-6091, a novel PEGylated colloidal gold-rhTNF nanomedicine. *Clin Cancer Res* 16(24):6139–6149
- Lim YT, Cho MY, Kim JK et al (2007) Plasmonic magnetic nanostructure for bimodal imaging and photonic-based therapy of cancer cells. *ChemBioChem* 8(18):2204–2209. doi:[10.1002/cbic.200700416](https://doi.org/10.1002/cbic.200700416)
- Lin YH, Tseng WL (2010) Ultrasensitive sensing of Hg²⁺ and CH₃Hg⁺ based on the fluorescence quenching of lysozyme Type VI-stabilized gold nanoclusters. *Anal Chem* 82(22):9194–9200. doi:[10.1021/ac101427y](https://doi.org/10.1021/ac101427y)
- Lin A, Lewinski N, Lee MH et al (2006) Reflectance spectroscopy of gold nanoshells: computational predictions and experimental measurements. *J Nanoparticle Res* 8(5):681–692
- Lin CAJ, Lee CH, Hsieh JT et al (2009a) Synthesis of fluorescent metallic nanoclusters toward biomedical application: recent progress and present challenges. *J Med Biol Eng* 29(6):76–283
- Lin CAJ, Yang TY, Lee CH et al (2009b) Synthesis, characterization, and bioconjugation of fluorescent gold nanoclusters toward biological labeling applications. *ACS Nano* 3(2):395–401. doi:[10.1021/nm800632j](https://doi.org/10.1021/nm800632j)
- Lin CAJ, Lee CH, Hsieh JT et al (2010) Synthesis and surface modification of highly fluorescent gold nanoclusters and their exploitation for cellular labeling. *Proc SPIE* 7575. doi:[10.1117/12.841540](https://doi.org/10.1117/12.841540)
- Lin H, Li L, Lei C et al (2013a) Immune-independent and label free fluorescent assay for Cystatin C detection based on protein stabilized Au nanoclusters. *Biosens Bioelectron* 41(1):256–261
- Lin J, Zhou Z, Li Z et al (2013b) Biomimetic one-pot synthesis of gold nanoclusters/nanoparticles for targeted tumor cellular dual-modality imaging. *Nanoscale Res Lett* 8(1):170. doi:[10.1186/1556-276X-8-170](https://doi.org/10.1186/1556-276X-8-170)
- Link S, Beeby A, FitzGerald S et al (2002) Visible to infrared luminescence from a 28-atom gold cluster. *J Phys Chem B* 106(13):3410–3415. doi:[10.1021/jp014259v](https://doi.org/10.1021/jp014259v)
- Liu CL, Wu HT, Hsiao YH et al (2011) Insulin-directed synthesis of fluorescent gold nanoclusters: preservation of insulin bioactivity and versatility in cell imaging. *Angew Chem Int Ed* 50(31):7056–7060
- Liu G, Shao Y, Ma K et al (2012a) Synthesis of DNA-templated fluorescent gold nanoclusters. *Gold Bulletin* 45(2):69–74. doi:[10.1007/s13404-012-0049-6](https://doi.org/10.1007/s13404-012-0049-6)
- Liu G, Shao Y, Wu F et al (2012b) DNA-hosted fluorescent gold nanoclusters: sequence-dependent formation. *Nanotechnology* 24(1):015503. doi:[10.1088/0957-4484/24/1/015503](https://doi.org/10.1088/0957-4484/24/1/015503)

- Loo C, Lowery A, Halas N et al (2005) Immunotargeted nanoshells for integrated cancer imaging and therapy. *Nano Lett* 5(4):709–711. doi:[10.1021/nl050127s](https://doi.org/10.1021/nl050127s)
- Lu W, Zhang G, Zhang R et al (2010) Tumor site-specific silencing of NF-kappaB p65 by targeted hollow gold nanosphere-mediated photothermal transfection. *Cancer Res* 70:3177–3188. doi:[10.1158/0008-5472](https://doi.org/10.1158/0008-5472)
- Maffeo C, Yoo J, Comer J et al (2014) Close encounters with DNA. *J Phys Condense Matter* 26 (41):413101. doi:[10.1088/0953-8984/26/41/413101](https://doi.org/10.1088/0953-8984/26/41/413101)
- Maltzahn GV et al (2009) Computationally guided photothermal tumor therapy using long-circulating gold nanorod antennas. *Cancer Res* 69:3892–3900
- Marzan LML (2006) Tailoring surface plasmons through the morphology and assembly of metal nanoparticles. *Langmuir* 22(1):32–41. doi:[10.1021/la0513353](https://doi.org/10.1021/la0513353)
- Mayavan S, Dutta NK, Choudhury NR et al (2011) Self-organization, interfacial interaction and photophysical properties of gold nanoparticle complexes derived from resilin-mimetic fluorescent protein rec1-resilin. *Biomaterials* 32(11):2786–2796
- McCarthy JR, Bhaumik J, Karver MR et al (2010) Targeted nanoagents for the detection of cancers. *Mol Oncol* 4(6):511–528
- Medley CM, Smith JE, Tang Z et al (2008) Gold nanoparticle-based colorimetric assay for the direct detection of cancerous cells. *Anal Chem* 80:1067–1072
- Michalet X, Pinaud FF, Bentolila LA et al (2005) Quantum dots for live cells, in vivo imaging and diagnostics. *Science* 307(5709):538–544. doi:[10.1126/science.1104274](https://doi.org/10.1126/science.1104274)
- Mie G (1908) Beitrage zur Optik trüber Medien speziell kolloidaler Goldlösungen (contributions to the optics of diffuse media, especially colloid metal solutions). *Ann Phys* 25:377–445
- Muhammed MAH, Ramesh S, Sinha SS et al (2008) Two distinct fluorescent quantum clusters of gold starting from metallic nanoparticles by pH-dependent ligand etching. *Nano Res* 1(4):333–340. doi:[10.1007/s12274-008-8035-2](https://doi.org/10.1007/s12274-008-8035-2)
- Muhammed MAH, Verma PK, Pal SK et al (2009) Bright, NIR-emitting Au₂₃ from Au₂₅: characterization and applications including biolabeling. *Chem Eur J* 15:10110–10120. doi:[10.1002/chem.200901425](https://doi.org/10.1002/chem.200901425)
- Muhammed MAH, Verma PK, Pal SK et al (2010) Luminescent quantum clusters of gold in bulk by albumin-induced core etching of nanoparticles: metal ion sensing, metal-enhanced luminescence, and biolabeling. *Chem Eur J* 16(33):10103–10112. doi:[10.1002/chem.201000841](https://doi.org/10.1002/chem.201000841)
- Naik RR, Jones SE, Murray CJ et al (2004) Peptide templates for nanoparticle synthesis derived from polymerase chain reaction-driven phage display. *Adv Funct Mater* 14(1):25–30. doi:[10.1002/adfm.200304501](https://doi.org/10.1002/adfm.200304501)
- Nandini S, Nalini S, Sanetuntikul J et al (2014) Development of a simple bioelectrode for the electrochemical detection of hydrogen peroxide using *Pichia pastoris* catalase immobilized on gold nanoparticle nanotubes and polythiophene hybrid. *Analyst* 139(22):5800–5812
- Nandini S, Nalini S, Madhusudana Reddy MB et al (2016a) Synthesis of one-dimensional gold nanostructures and the electrochemical application of the nanohybrid containing functionalized graphene oxide for cholesterol biosensing. *Bioelectrochem* 110:79–90
- Nandini S, Nalini S, Madhusudana Reddy MB et al (2016b) A novel bioassay based biosensor-credible to abet preclinical evaluation of anticancer properties developed by gold nanoribbons. *RSC Adv* 6:60693–60703. doi:[10.1039/C6RA07501K](https://doi.org/10.1039/C6RA07501K)
- Nguyen QT, Tsien RY (2013) Fluorescence-guided surgery with live molecular navigation—a new cutting edge. *Nat Rev Cancer* 13:653–662. doi:[10.1038/nrc3566](https://doi.org/10.1038/nrc3566)
- O’Neal DP, Hirsch LR, Halas NJ et al (2004) Photo-thermal tumor ablation in mice using near infrared-absorbing nanoparticles. *Cancer Lett* 209(2):171–176
- Paciotti GF, Myer L, Weinreich D et al (2004) Colloidal gold: a novel nanoparticle vector for tumor directed drug delivery. *Drug Deliv* 11(3):169–183

- Peer D, Karp JM, Hong S et al (2007) Nanocarriers as an emerging platform for cancer therapy. *Nat Nanotechnol* 2:751–760. doi:[10.1038/nnano.2007.387](https://doi.org/10.1038/nnano.2007.387)
- Plascencia-Villa G, Torrente D, Marucho M et al (2015) Biodirected synthesis and nanostructural characterization of anisotropic gold nanoparticles. *Langmuir* 31:3527–3536. doi:[10.1021/acs.langmuir.5b00084](https://doi.org/10.1021/acs.langmuir.5b00084)
- Polavarapu L, Manna M, Xu QH (2011) Biocompatible glutathione capped gold clusters as one- and two-photon excitation fluorescence contrast agents for live cells imaging. *Nanoscale* 3:429–434. doi:[10.1039/C0NR00458H](https://doi.org/10.1039/C0NR00458H)
- Popovtzer R, Agrawal A, Kotov NA et al (2008) Targeted gold nanoparticles enable molecular CT imaging of cancer. *Nano Lett* 8:4593–4596. doi:[10.1021/nl8029114](https://doi.org/10.1021/nl8029114)
- Prakash M, Shetty MS, Tilak P et al (2009) Total thiols: biomedical importance and their alteration in various disorders. *Online J Health Allied Scs* 8(2):2
- Pricker SP (1996) Medical uses of gold compounds: past, present and future. *Gold Bull* 29(2): 53–60
- Qian X, Peng XH, Ansari DO et al (2008) In vivo tumor targeting and spectroscopic detection with surface-enhanced Raman nanoparticle tags. *Nature Biotechnol* 26:83–90. doi:[10.1038/nbt1377](https://doi.org/10.1038/nbt1377)
- Qian H, Zhu Y, Jin R (2009) Size-Focusing synthesis, optical and electrochemical properties of monodisperse Au₃₈(SC₂H₄Ph)₂₄ nanoclusters. *ACS Nano* 3(11):3795–3803. doi:[10.1021/nl901137h](https://doi.org/10.1021/nl901137h)
- Qiao J, Mu X, Qi L et al (2013) Folic acid-functionalized fluorescent gold nanoclusters with polymers as linkers for cancer cell imaging. *Chem Commun* 49:8030–8032. doi:[10.1039/C3CC44256J](https://doi.org/10.1039/C3CC44256J)
- Qu X, Li Y, Li L et al (2015) Fluorescent gold nanoclusters: synthesis and recent biological application. *J Nanomater* 2015:4. doi:[10.1155/2015/784097](https://doi.org/10.1155/2015/784097)
- Quinn BM, Liljeroth P, Ruiz V et al (2003) Electro chemical resolution of 15 oxidation states for monolayer protected gold nanoparticles. *J Am Chem Soc* 125(22):6644–6645
- Retnakumari R, Jayasimhan J, Chandran P et al (2011) CD33 monoclonal antibody conjugated Au cluster nano-bioprobe for targeted flow-cytometric detection of acute myeloid leukaemia. *Nanotechnology* 22(28):285102
- Roco MC (2003) Nanotechnology: convergence with modern biology and medicine. *Curr Opin Biotechnol* 14(3):337–346
- Roy S, Baral A, Bhattacharjee R et al (2015) Preparation of multi-coloured different sized fluorescent gold clusters from blue to NIR, structural analysis of the blue emitting Au₇ cluster, and cell-imaging by the NIR gold cluster. *Nanoscale* 7:1912–1920. doi:[10.1039/C4NR04338C](https://doi.org/10.1039/C4NR04338C)
- Sahoo AK, Banerjee S, Ghosh SS et al (2014) Simultaneous RGB emitting Au nanoclusters in chitosan nanoparticles for anticancer gene theranostics. *ACS Appl Mater Interfaces* 6(1):712–724. doi:[10.1021/am4051266](https://doi.org/10.1021/am4051266)
- Saravanakumar G, Kim K, Park JH et al (2009) Current status of nanoparticle-based imaging agents for early diagnosis of cancer and atherosclerosis. *J Biomed Nanotechnol* 5(1):20–35
- Sardar R, Funston AM, Mulvaney P et al (2009) Gold nanoparticles: past, present, and future. *Langmuir* 25:13840–13851
- Sauerbeck C, Haderlein M, Schurer B et al (2014) Shedding light on the growth of gold nanoshells. *ACS Nano* 8(3):3088–3096
- Schaaff TG, Shafiqullin MN, Khoury JT et al (1997) Isolation of smaller nanocrystal Au molecules: robust quantum effects in optical spectra. *J Phys Chem B* 101:7885–7891
- Sekhon BS (2014) Nanotechnology in agri-food production: an overview. *Nanotechnol Sci Appl* 7:31–53. doi:[10.2147/NSA.S39406](https://doi.org/10.2147/NSA.S39406)
- Selvaprakash K, Chen YC (2014) Using protein-encapsulated gold nanoclusters as photoluminescent sensing probes for biomolecules. *Biosens Bioelectron* 61:88–94. doi:[10.1016/j.bios.2014.04.055](https://doi.org/10.1016/j.bios.2014.04.055)
- Shan J, Tenhu H (2007) Recent advances in polymer protected gold nanoparticles: synthesis, properties and applications. *Chem Commun* 44:4580–4598
- Shang L, Dong SJ, Nienhaus GU (2011a) Ultra-small fluorescent metal nanoclusters: synthesis and biological applications. *Nano Today* 6(4):401–418

- Shang L, Dörlich RM, Brandholt S et al (2011b) Facile preparation of water-soluble fluorescent gold nanoclusters for cellular imaging applications. *Nanoscale* 3(5):2009–2014. doi:[10.1039/c0nr00947d](https://doi.org/10.1039/c0nr00947d)
- Shervani Z, Yamamoto Y (2011) Carbohydrate-directed synthesis of silver and gold nanoparticles: effect of the structure of carbohydrates and reducing agents on the size and morphology of the composites. *Carbohydr Res* 346(5):651–658. doi:[10.1016/j.carres.2011.01.020](https://doi.org/10.1016/j.carres.2011.01.020)
- Shi X, Ganser TR, Sun K et al (2006) Characterization of crystalline dendrimer-stabilized gold nanoparticles. *Nanotechnology* 17:1072–1078. doi:[10.1088/0957-4484/17/4/038](https://doi.org/10.1088/0957-4484/17/4/038)
- Shibu ES, Pradeep T (2011) Quantum clusters in cavities: trapped Au15 in cyclodextrins. *Chem Mater* 23(4):989–999. doi:[10.1021/cm102743y](https://doi.org/10.1021/cm102743y)
- Shibu ES, Radha B, Verma PK et al (2009) Functionalized Au22 clusters: synthesis, characterization, and patterning. *ACS Appl Mater Interfaces* 1(10):2199–2210. doi:[10.1021/am900350r](https://doi.org/10.1021/am900350r)
- Shichibu Y, Negishi Y, Tsunoyama H et al (2007) Extremely high stability of glutathionate-protected Au 25 clusters against core etching. *Small* 3(5):835–839
- Shukla MK, Dubey M, Zakar E et al (2009) DFT investigation of the interaction of gold nanoclusters with nucleic acid base guanine and the Watson-Crick guanine-cytosine base pair. *J Phys Chem C* 113(10):3960–3966
- Sivasubramanian M, Hsia Y, Lo LW (2014) Nanoparticle-facilitated functional and molecular imaging for the early detection of cancer. *Front Mol Biosci* 1:15. doi:[10.3389/fmolb.2014.00015](https://doi.org/10.3389/fmolb.2014.00015)
- Smith AM, Dave S, Nie SM et al (2006) Multicolor quantum dots for molecular diagnostics of cancer. *Expert Rev Mol Diagn* 6(2):231–244
- Sokolov K, Follen M, Aaron J et al (2003) Real-time vital optical imaging of precancer using anti-epidermal growth factor receptor antibodies conjugated to gold nanoparticles. *Cancer Res* 63:1999–2004
- Song J, Zhou J, Duan H (2012) Self-assembled plasmonic vesicles of SERS-encoded amphiphilic gold nanoparticles for cancer cell targeting and traceable intracellular drug delivery. *J Am Chem Soc* 134(32):13458–13469
- Song JT, Yang XQ, Zhang XS et al (2015) Facile synthesis of gold nanospheres modified by positively charged mesoporous silica, loaded with near-infrared fluorescent dye, for in vivo X-ray computed tomography and fluorescence dual mode imaging. *ACS Appl Mater Interfaces* 7:17287–17297. doi:[10.1021/acsami.5b04359](https://doi.org/10.1021/acsami.5b04359)
- Srinivasan M, Rajabi M, Mousa SA (2015) Multifunctional nanomaterials and their applications in drug delivery and cancer therapy. *Nanomaterials* 5(4):1690–1703
- Stern JM, Stanfield J, Kabbani W et al (2008) Selective prostate cancer thermal ablation with laser activated gold nanoshells. *J Urol* 179(2):748–753
- Takahashi H, Niidome T, Nariai A et al (2006) Gold nanorod-sensitized cell death: microscopic observation of single living cells irradiated by pulsed near-infrared laser light in the presence of gold nanorods. *Chem Lett* 35(5):500–501
- Tan YN, Lee JY, Wang DIC (2010) Uncovering the design rules for peptide synthesis of metal nanoparticles. *J Am Chem Soc* 132(16):5677–5686. doi:[10.1021/ja907454f](https://doi.org/10.1021/ja907454f)
- Tao Y, Lin Y, Ren J et al (2013) A dual fluorometric and colorimetric sensor for dopamine based on BSA-stabilized Au nanoclusters. *Biosens Bioelectron* 42(1):41–46
- Thygesen MB, Jensen KJ (2015) Carbohydrate-modified gold nanoparticles. In: Stine KJ (ed) *Carbohydrate nanotechnology*. Wiley, Hoboken, NJ
- Triulzi RC, Micic M, Giordani S et al (2006) Immunoassay based on the antibody-conjugated PAMAM-dendrimer-gold quantum dot complex. *Chem Commun* 48:5068–5070
- Tsoi KM, Dai Q, Alman BA et al (2013) Are quantum dots toxic? Exploring the discrepancy between cell culture and animal studies. *Acc Chem Res* 46(3):662–671
- Tu X, Chen W, Guo X (2011) Facile one-pot synthesis of near infrared luminescent gold nanoparticles for sensing copper (II). *Nanotechnology* 22(9):095701. doi:[10.1088/0957-4484/22/9/095701](https://doi.org/10.1088/0957-4484/22/9/095701)

- Vankayala R, Kuo CL, Nuthalapati K et al (2015) Nucleus-targeting gold nanoclusters for simultaneous *in vivo* fluorescence imaging, gene delivery, and NIR-light activated photodynamic therapy. *Adv Funct Mater* 25(37):5934–5945. doi:[10.1002/adfm.201502650](https://doi.org/10.1002/adfm.201502650)
- Visaria R, Griffin R, Williams B et al (2006) Enhancement of tumor thermal therapy using gold nanoparticle assisted tumor necrosis factor- α delivery. *Mol Cancer Ther* 5(4):1014–1020
- Wang G, Huang T, Murray RW et al (2005) Near-IR luminescence of monolayer-protected metal clusters. *J Am Chem Soc* 127(3):812–813
- Wang HH, Lin CAJ, Lee CH et al (2011a) Fluorescent gold nanoclusters as a biocompatible marker for *in vitro* and *in vivo* tracking of endothelial cells. *ACS Nano* 5(6):4337–4344. doi:[10.1021/nn102752a](https://doi.org/10.1021/nn102752a)
- Wang Y, Chen J, Irudayaraj J et al (2011b) Nuclear targeting dynamics of gold nanoclusters for enhanced therapy of HER2 β breast cancer. *ACS Nano* 5(12):9718–9725
- Wang J, Zhang G, Li Q et al (2013) *In vivo* self-bio-imaging of tumors through *in situ* biosynthesized fluorescent gold nanoclusters. *Sci Rep* 3:1157. doi:[10.1038/srep01157](https://doi.org/10.1038/srep01157)
- Wang YQ, Zhao T, He XW et al (2014) A novel core-satellite CdTe/Silica/Au NCs hybrid sphere as dual-emission ratiometric fluorescent probe for Cu²⁺. *Biosens Bioelectron* 51:40–46. doi:[10.1016/j.bios.2013.07.028](https://doi.org/10.1016/j.bios.2013.07.028)
- Wei H, Wang Z, Yang L et al (2010) Lysozyme stabilized gold fluorescent cluster: synthesis and application as Hg₂⁺ sensor. *Analyst* 135:1406–1410. doi:[10.1039/C0AN00046A](https://doi.org/10.1039/C0AN00046A)
- Wei H, Wang Z, Zhang J et al (2011) Time dependent, protein-directed growth of gold nanoparticles within a single crystal of lysozyme. *Nat Nanotechnol* 6:93–97. doi:[10.1038/nnano.2010.280](https://doi.org/10.1038/nnano.2010.280)
- Weissleder R (2002) Scaling down imaging: molecular mapping of cancer in mice. *Nat Rev Cancer* 2(1):11–18
- Wen F, Dong Y, Feng L et al (2011) Horseradish peroxidase functionalized fluorescent gold nanoclusters for hydrogen peroxide sensing. *Anal Chem* 83(4):1193–1196
- Wen Q, Gu Y, Tang LJ et al (2013) Peptide-templated gold nanocluster beacon as a sensitive, label-free sensor for protein posttranslational modification enzymes. *Anal Chem* 85(24):11681–11685. doi:[10.1021/ac403308b](https://doi.org/10.1021/ac403308b)
- West AL, Griep MH, Cole DP et al (2014) DNase 1 retains endodeoxyribonuclease activity following gold nanocluster synthesis. *Anal Chem* 86(15):7377–7382. doi:[10.1021/ac5005794](https://doi.org/10.1021/ac5005794)
- Wilcoxon JP, Martin JE, Parsapour F et al (1998) Photoluminescence from nano size gold clusters. *J Chem Phys* 108(21):9137–9143
- Wu Z, Jin R (2010) On the ligand's role in the fluorescence of gold nanoclusters. *Nano Lett* 10(7):2568–2573
- Wu X, He X, Wang K et al (2010) Ultrasmall near-infrared gold nanoclusters for tumor fluorescence imaging *in vivo*. *Nanoscale* 2:2244–2249. doi:[10.1039/C0NR00359J](https://doi.org/10.1039/C0NR00359J)
- Xavier PL, Chaudhari K, Verma PK et al (2010) Luminescent quantum clusters of gold in transferrin family protein, lactoferrin exhibiting FRET. *Nanoscale* 2(12):2769–2776. doi:[10.1039/c0nr00377h](https://doi.org/10.1039/c0nr00377h)
- Xiao Y, Hong H, Javadi A et al (2012) Gold nanorods conjugated with doxorubicin and cRGD for combined anticancer drug delivery and PET imaging. *Theranostics* 2(8):757–768
- Xie J, Lee JY, Wang DIC et al (2007) Silver nanoplates: from biological to biomimetic synthesis. *ACS Nano* 1(5):429–439
- Xie J, Zheng Y, Ying JY (2009) Protein-directed synthesis of highly fluorescent gold nanoclusters. *J Am Chem Soc* 131(3):888–889
- Xie J, Zheng Y, Ying JY (2010) Highly selective and ultrasensitive detection of Hg²⁺ based on fluorescence quenching of Au nanoclusters by Hg²⁺-Au⁺ interactions. *Chem Commun* 46:961–963. doi:[10.1039/B920748A](https://doi.org/10.1039/B920748A)
- Xu HX, Suslick KS (2010) Water-soluble fluorescent silver nanoclusters. *Adv Mater* 22(10):1078–1082

- Yabu H (2011) One-pot synthesis of blue light-emitting Au nanoclusters and formation of photo-patternable composite films. *Chem Commun* 47(4):1196–1197. doi:[10.1039/c0cc03539d](https://doi.org/10.1039/c0cc03539d)
- Yang X, Stein EW, Ashkenazi S et al (2009) Nanoparticles for photoacoustic imaging. *WIREs Nanomed Nanobiotechnol* 1:360–368. doi:[10.1002/wnan.42](https://doi.org/10.1002/wnan.42)
- Yang QF, Liu JY, Chen HP et al (2011a) Preparation of noble metallic nanoclusters and its application in biological detection. *Prog Chem* 23(5):880–892
- Yang X, Shi M, Zhou R et al (2011b) Blending of HAuCl₄ and histidine in aqueous solution: a simple approach to the Au₁₀ cluster. *Nanoscale* 3(6):2596–2601. doi:[10.1039/c1nr10287g](https://doi.org/10.1039/c1nr10287g)
- Yang X, Luo Y, Zhuo Y et al (2014) Novel synthesis of gold nanoclusters templated with L-tyrosine for selective analyzing tyrosinase. *Anal Chim Acta* 840:87–92. doi:[10.1016/j.aca.2014.05.050](https://doi.org/10.1016/j.aca.2014.05.050)
- You J, Zhang G, Li C (2010) Exceptionally high payload of doxorubicin in hollow gold nanospheres for near-infrared light-triggered drug release. *ACS Nano* 4(2):1033–1041
- You J, Zhang R, Zhan G et al (2012) Photothermal-chemotherapy with doxorubicin-loaded hollow gold nanospheres: a platform for near-infrared light-triggered drug release. *J Control Release* 158(2):319–328
- Yu M, Zhou C, Liu J et al (2011) Luminescent gold nanoparticles with pH-dependent membrane adsorption. *J Am Chem Soc* 133(29):11014–11017. doi:[10.1021/ja201930p](https://doi.org/10.1021/ja201930p)
- Yu MK, Park J, Jon S (2012) Targeting strategies for multifunctional nanoparticles in cancer imaging and therapy. *Theranostics* 2(1):3–44
- Zamboni WC, Torchilin V, Patri A et al (2012) Best practices in cancer nanotechnology: perspective from NCI nanotechnology alliance. *Clin Cancer Res* 18(12):3229–3241. doi:[10.1158/1078-0432.CCR-11-2938](https://doi.org/10.1158/1078-0432.CCR-11-2938)
- Zavaleta CL, Smith BR, Walton I et al (2009) Multiplexed imaging of surface enhanced raman scattering nanotags in living mice using noninvasive raman spectroscopy. *Proc Natl Acad Sci* 106(32):13511–13516. doi:[10.1073/pnas.0813327106](https://doi.org/10.1073/pnas.0813327106)
- Zhang L, Wang E (2014) Metal nanoclusters: new fluorescent probes for sensors and bioimaging. *Nano Today* 9(1):132–157
- Zhang XD, Chen J, Luo Z et al (2013) Enhanced tumor accumulation of sub-2 nm gold nanoclusters for cancer radiation therapy. *Adv Healthcare Mater* 3(1):133–141
- Zhang J, Yuan Y, Wang Y et al (2015) Microwave-assisted synthesis of photoluminescent glutathione-capped Au/Ag nanoclusters: a unique sensor-on-a-nanoparticle for metal ions, anions, and small molecules. *Nano Res* 8(7):2329–2339. doi:[10.1007/s12274-015-0743-9](https://doi.org/10.1007/s12274-015-0743-9)
- Zheng J (2005) Fluorescent noble metal nanoclusters. Ph D Thesis, Georgia Institute of Technology, Atlanta
- Zheng J, Petty JT, Dickson RM (2003) High quantum yield blue emission from water soluble Au₈ nanodots. *J Am Chem Soc* 125(26):7780–7781
- Zheng J, Zhang CW, Dickson RM (2004) Highly fluorescent, water-soluble, size-tunable gold quantum dots. *Phys Rev Lett* 93(7):077402. doi:[10.1103/PhysRevLett.93.077402](https://doi.org/10.1103/PhysRevLett.93.077402)
- Zheng J, Nicovich PR, Dickson RM (2007) Highly fluorescent noble metal quantum dots. *Annu Rev Phys Chem* 58(1):409–431
- Zheng CF, Zheng MB, Gong P et al (2012) Indocyanine green-loaded biodegradable tumor targeting nanoprobe for in vitro and in vivo imaging. *Biomaterials* 33(22):5603–5609
- Zhou Z, Zhang C, Qian Q et al (2013) Folic acid-conjugated silica capped gold nanoclusters for targeted fluorescence/X-ray computed tomography imaging. *J Nanobiotechnol* 11:17. doi:[10.1186/1477-3155-11-17](https://doi.org/10.1186/1477-3155-11-17)